ISSN 0869-5938, Stratigraphy and Geological Correlation, 2012, Vol. 20, No. 3, pp. 261–294. © Pleiades Publishing, Ltd., 2012.
Original Russian Text © A.Yu. Guzhikov, V.V. Arkad'ev, E.Yu. Baraboshkin, M.I. Bagaeva, V.K. Piskunov, S.V. Rud'ko, V.A. Perminov, A.G. Manikin, 2012, published in Stratigrafiya. Geologicheskaya Korrelyatsiya, 2012, Vol. 20, No. 3, pp. 35–71.

New Sedimentological, Bio-, and Magnetostratigraphic Data on the Jurassic–Cretaceous Boundary Interval of Eastern Crimea (Feodosiya)

A. Yu. Guzhikov[a], V. V. Arkad'ev[b], E. Yu. Baraboshkin[c], M. I. Bagaeva[a], V. K. Piskunov[d], S. V. Rud'ko[d], V. A. Perminov[e], and A. G. Manikin[a]

[a]*Chernyshevsky Saratov State University, ul. Astrakhanskaya 83, Saratov, 410012 Russia*
E-mail: aguzhikov@yandex.ru
[b]*St. Petersburg State University, Universitetskaya nab. 7/9, St. Petersburg, 199034 Russia*
[c]*Lomonosov Moscow State University, Leninskie Gory, Moscow, 119992 Russia*
[d]*Geological Institute, Russian Academy of Sciences, Pyzhevskii per. 7, Moscow, 119017 Russia*
[e]*Center of Ecological–Naturalistic Creativity of Students "Intellekt", Feodosiya, Ukraine*

Received April 13, 2011; in final form September 19, 2011

Abstract—The first compiled composite section comprises continuous succession of upper Tithonian–lower Berriasian strata (Jacobi Zone) from different isolated outcrops of the Feodosiya area. Based on new magnetostratigraphic and sedimentological data, the paleomagnetic section is correlated with succession of M20r, M19n, M19r, M18b chrons and M18n.1r Subchron ("Brodno"). The thorough complex bio- and magnetostratigraphic correlation of the upper Tithonian–lower Berriasian interval (Jacobi Zone) carried out through the Western Tethys and Eastern Paratethys provided grounds for first defining age analogs of the Durangites Zone in the Crimean Mountains and specifying location of the boundary between the Jurassic and Cretaceous systems, as well as for determining late Tithonian age of strata in the Dvuyakornaya Bay section barren of fossils.

Keywords: Jurassic–Cretaceous boundary, Tithonian, Berriasian, Crimea, sedimentology, ammonites, biostratigraphy, magnetostratigraphy, paleomagnetism, magnetic polarity, magnetic chrons.

DOI: 10.1134/S0869593812030045

INTRODUCTION

The zonal and infrazonal correlation of Tithonian–Berriasian strata through the Western Tethys and Eastern Peri-Tethys including the Crimean Mountains, and tracing the Jurassic–Cretaceous boundary in the latter, placed by some researchers at the base of the Jacobi Zone in the Tethyan realm (Reboulet et al., 2009), remains one of the problems of the present-day stratigraphy. Until recently, its solution was complicated by the rarity of ammonite finds in the Tithonian–Berriasian sediments of Crimea, lack of sedimentological data, which would indicate the completeness of the section, magnetostratigraphic, isotopic, and chemostratigraphic characteristics, and other materials required for substantiating boundaries between stratigraphic units at the present level of knowledge.

In this work, we give the first description of the composite section, which comprises a continuous succession of strata from different outcrops of the clayey–carbonate flyschoid Dvuyakornaya Formation located in Black Sea cliffs in the Cape Feodosiiskii, Cape Svyatogo Il'i, and Dvuyakornaya Bay areas on the southern outskirts of Feodosiya (Fig. 1). New paleontological (finds of ammonites), sedimentological, and magnetostratigraphic data derived from these sections led to significant progress in detailed interregional correlations of upper Tithonian–lower Berriasian strata with their coeval analogs in the Western Tethyan realm.

To exclude possible misinterpretations and errors in coordination of data obtained by different methods, the section was sampled in the bed-by-bed manner simultaneously with geological description and paleontological analysis. This procedure included selection of oriented samples for paleomagnetic studies, the results of which are considered in this article, and samples for the micropaleontological (calpionellids), lithological–mineralogical–roentgenographic, and isotopic analyses, which are now in progress. In total, 240 stratigraphic levels of a section approximately 350 m thick were sampled.

All the authors took part in sampling and section investigations: E.Yu. Baraboshkin, V.K. Piskunov, and S.V. Rud'ko conducted sedimentological studies; A.Yu. Guzhikov and M.I. Bagaeva collected and ana-

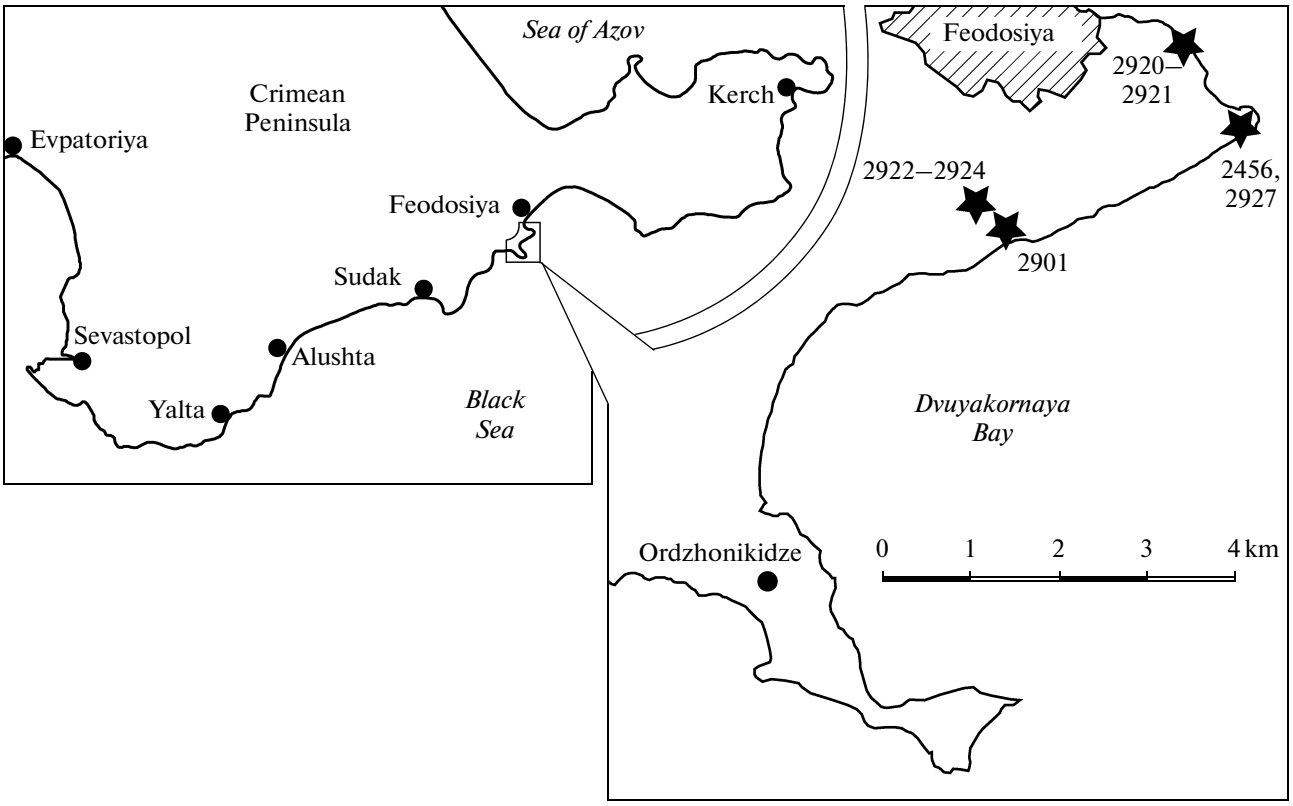

Fig. 1. Schematic location of upper Tithonian and lower Berriasian outcrops near Feodosiya (asterisks).
Outcrops 2901 and 2922–2924 are located in the Dvuyakornaya Bay; outcrops 2456 and 2927 are in the Cape Svyatogo Il'i area; outcrops 2920 and 2921 are in the Cape Feodosiiskii area.

lyzed paleomagnetic data; V.V. Arkad'ev and E.Yu. Baraboskin identified and described ammonites.

BRIEF REVIEW OF THE SECTION INVESTIGATION HISTORY

The history of investigation of the Jurassic–Cretaceous boundary section in the Feodosiya area and, primarily, its paleontological finds, starting in the late 19th century (Sokolov, 1886; Retowski, 1893; and others) was reviewed in a recent publication (Arkad'ev et al., 2006). The most complete description of the section was provided by Muratov (1937), who noted the gradual transition between the Jurassic and Cretaceous strata and conditionally placed the boundary between them at the base of a 1-m-thick conglomerate-like limestone bed observable in the Cape Svyatogo Il'i section (Muratov, 1937, p. 57).

In 1954–1956, the Lower Cretaceous sections of Crimea and their organic remains were studied by a team of geologists from the Moscow State University under supervision of V.V. Drushchits, who was the first to describe in detail the "Feodosiya-type" Berriasian section with their transition to the Tithonian strata and provide zonal subdivision of these sediments. The Berriasian Stage was initially included into the Valanginian (Drushchits and Kudryavtsev, 1960). Subsequently, following Muratov (1937), the base of a thick (1.25 m) conglomerate-like limestone bed was accepted to represent the Tithonian–Berriasian boundary based on the replacement of the ammonite assemblage with *Substreblites zonaria* and *Cyrtosiceras macrotela* by their assemblage with *Pseudosubplanites euxinus, P. ponticus, Himalayites cortazari*, and others (Drushchits, 1975, p. 338). The last author attributed the Berriasian in its present-day understanding partly to the middle Tithonian and partly to the upper Tithonian (Drushchits, 1969, 1975). The main distribution features of different faunal and floral groups in this section were considered by the following researchers: foraminifers by T.N. Gorbachik (1969), palynological complexes by S.B. Kuvaeva (Kuvaeva and Yanin, 1973), bivalves by B.T. Yanin (Yanin and Smirnova, 1981), brachiopods by T.N. Smirnova and S.V. Lobacheva (Smirnova, 1962; Yanin and Smirnova, 1981; Lobacheva and Smirnova, 2002, 2006). The distribution of different organic remains and trace fossils in the Lower Cretaceous sections of Crimes, the Feodosiya one included, was summarized by Gorbachik et al. (1970).

In the 1970s, the Feodosiya section was visited by K.I. Kuznetsova, N.P. Mikhailov, and E.A. Uspenskaya. Its member-by-member description (beginning from the upper Tithonian) and analysis of foramin-

iferal assemblages with the zonal subdivision are provided in (Kuznetsova and Gorbachik, 1985). The foraminiferal assemblages are correlated with the Drushchits ammonite succession (Kuznetsova and Gorbachik, 1985). Following their predecessors, these authors accepted the base of the conglomerate-like limestone member to correspond to the lower boundary of the confirmed Berriasian, although it is underlain by a thick (143 m) sequence of uncertain stratigraphic position ("upper Tithonian–lower Berriasian").

In the 1980s, the section was repeatedly visited by many geologists. For example, Sazonova and Sazonov (1974) proposed a new ammonite zonation for the latter and subsequently (Sazonova and Sazonov, 1984) reported on calpionellid assemblages from the same section. Unfortunately, these finds remain uncorrelated with the section and cannot be taken into consideration.

Simultaneously, geologists from the All-Union (now All-Russian) Institute of Geology (VSEGEI) carried out complex investigations of the Berriasian in the Crimean Mountains including the Feodosiya area (Bogdanova et al., 1981). These researchers examined in detail the Cape Svyatogo Il'i section and defined there the Pseudoplanites ponticus–P. grandis Zone, the basal Berriasian unit (Bogdanova et al., 1984). They conditionally attributed a clayey sequence intercalated by thin beds of ferruginate sandstones underlying the thick conglomerate-like limestone member to the Tithonian. They did not find any characteristic Tithonian ammonites, since sections in the Dvyyakornaya Bay other than those in the Cape Svyatogo Il'i area were inaccessible for study.

V.V. Arkad'ev examined the Feodosiya section annually since 2001, and he managed, as sections of the Dvuyakornaya Formation in the eponymous bay became accessible, first, to describe the lower part of the last unit and, second, to find ammonites in this section. In 2002, he found the first remains of the upper Tithonian ammonite species *Oloriziceras* cf. *schneidi* Tavera (Arkad'ev, 2004). Subsequently, he developed a preliminary zonal scale for the Jurassic–Cretaceous boundary interval of Eastern Crimea with substantiated analogs of the upper Tithonian Microcanthum Zone (Arkad'ev et al., 2006; Arkad'ev, 2008).

The investigation of microfossils from the Jurassic–Cretaceous boundary sediments was continued by A.A. Fedorova (Arkad'ev et al., 2006), who defined successive upper Tithonian–lower Berriasian zonal foraminiferal assemblages similar to their succession established by previous researchers (Kuznetsova and Gorbachik, 1985) and reliably correlated them with the ammonite zonation. Yu.N. Savel'eva and E.M. Tesakova analyzed the distribution of ostracods in the Cape Svyatogo Il'i and Dvuyakornaya Bay sections (Arkad'ev and Savel'eva, 2002; Arkad'ev, 2003; Arkad'ev et al., 2004, 2006; Tesakova et al., 2004; Tesakova and Savel'eva, 2005). These investigations revealed highly diverse ostracods in these sections (over 100 species, of which several tens of forms are new) and substantial differences between their upper Jurassic and Berriasian assemblages. O.V. Shurekova is now analyzing dinocysts from the Feodosiya section (results not yet published). In 2009–2010, calpionellids were first studied from the Dvuyakornaya Formation section in the eponymous bay (Shchennikova and Arkad'ev, 2009; Platonov and Arkad'ev, 2011). E.S. Platonov preliminarily identified *Calpionellites* sp. from a member with the ammonite *Paraulacosphinctes* cf. *transitorius*, the stratigraphic range of which is limited to the Berriasian–Hauterivian, and *Remaniella* sp. (upper Tithonian–Hauterivian) from a member with the ammonite *Neoperisphinctes* cf. *falloti*. In 2010, samples were collected from every limestone bed of the Tithonan–Berriasian interval in the Dvuyakornaya Bay section. From these samples, 400 thin sections were prepared for defining calpionellids; their examination is in progress.

Table 1 presents information on the knowledge and zonal subdivision of the Feodosiya section based on different faunal and floral groups.

In the late 1980s, geologists from the Institute of Physics of the Earth, USSR Academy of Science (now IFZ RAN) together with their colleagues from the Institute of Mineral Resources (Ministry of Geology of UkrSSR) carried out paleomagnetic studies of Mesozoic rocks in the Crimean Mountains to specify the geodynamic history of the region. During these studies, samples were also taken from the Tithonian–Beriasian interval of the Dvuyakornaya Bay section (Pecherskii and Safonov, 1993). Despite the uncertain position of these samples in the section, the data obtained are important for magnetostratigraphic interpretations and substantiation of remanent magnetization age. In 2004, O.M. Yampol'skaya and M.V. Pimenov, geologists from the Saratov State University, conducted detailed paleomagnetic sampling in the Cape Svyatogo Il'i section (Yampol'skaya et al., 2006, 2009). During the magnetostratigraphic investigation of the Dvuyakornaya Bay section carried out by paleomagnetologists from the same university, Arkad'ev (2011), who took part in these works, found upper Tithonian ammonite species *Paraulacosphinctes* cf. *transitorius* (Oppel) and *P.* cf. *senoides* Tavera. Based on the complex analysis of new bio- and magnetostratigraphic data, analogs of the Tithonian Durangites Zone was defined (Arkad'ev et al., 2010). In 2010, complex investigations of Tithonian–Berriasian sections in the Feodosiya area were continued and expanded based on the detailed sedimentological study by E.Yu. Baraboshkin, V.K. Piskunov, and S.V. Rud'ko. These works resulted in the continuous bed-by-bed sampling of the entire upper Tithonian and Jacobi Zone section in the Dvuyakornaya Bay and Cape Feodosiiskii areas, which duplicates the Cape Svyatogo Il'i section, and ammonite finds from levels which were previously not known to contain fossils. The section was sampled in a sample-in-sample manner for paleomagnetic, micropaleontological (calpi-

Table 1. The extent of knowledge and zonal subdivision of the Feodosiya section based on different faunal and floral groups

Member	Stage	Substage	Palynological complex (Kuvaeva and Yanin, 1973)	Bivalves (Yanin and Smirnova, 1981)	Brachiopod beds (Lobacheva and Smirnova, 2006)	Foraminiferal zone, beds (Arkad'ev et al., 2006)	Ostracod beds (Arkad'ev et al., 2006)	Nannofossil zones (Matveev, 2009, 2010)	Ammonite zone/subzone/beds (Arkad'ev et al., 2006)		Ammonite zone/subzone/beds (this work)	
									Subzone/beds	Zone	Subzone/beds	Zone
12	Berriasian	Lower	I (bs1): spores (1.5–6%), pollen (94–98.5%), dominant *Classopollis* sp. (80–90%), Ginkgoales (0.5–3%), coniferous (0–5%)	*Amusium sokolovi* Ret.	Tonasirhynchia janini Beds	Textularia cerimica–Belorussiella taurica Beds	Raymoorea peculiaris–Eucytherura ardescae Beds	Nannoconus steinmannii–Lithraphidites carniolensis	Pseudosubplanites grandis	Berriasella jacobi	Pseudosubplanites grandis	Berriasella jacobi
11						Frondicularia cuspidiata–Saracenaria inflanta			Berriasella jacobi		Berriasella jacobi	
10						Protopeneroplis ultragranulatus–Siphoninella antiqua						
9	Tithonian	Upper	?	?	?	Anchispirocyclina lusitanica–Melathrokerion spirialis	Cytherelloidea tortuosa–Palaeocytheridea grossi Beds	Stephanilithion bigoti	?		?	
8												
7												
6												
5									Paraulacosphinctes cf. transitorius Beds	Micracanthum	Paraulacosphinctes transitorius Beds	Duranglites
4												
3												
2									Oloriziceras cf. schneidi Beds		Oloriziceras cf. schneidi Beds	Micracanthum
1												

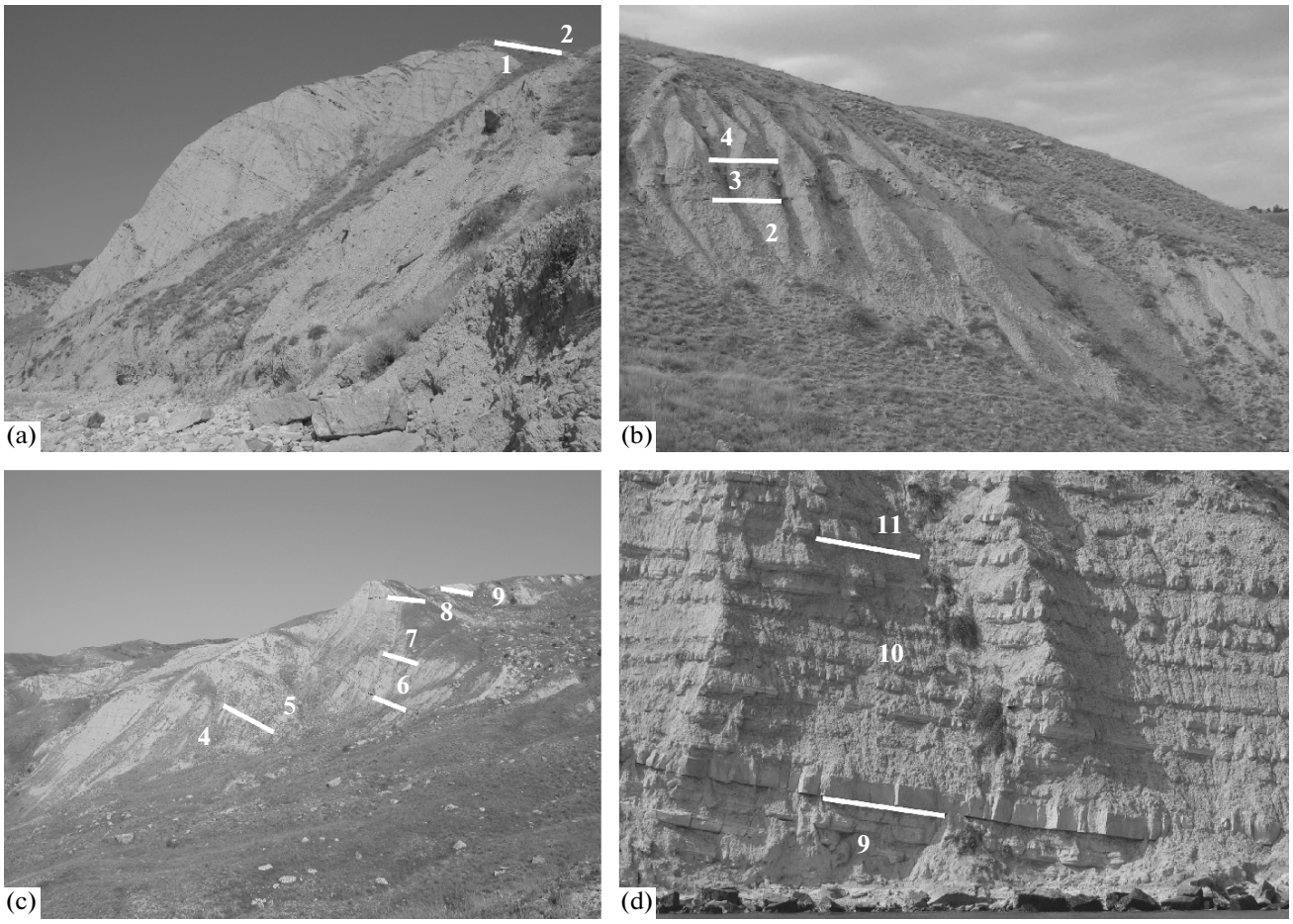

Fig. 2. Outcrops 2901 (a, b) and 2922–2924 (c) in the Dvuyakornaya Bay; outcrops 2920 and 2921 (d) in the Cape Feodosiiskii area. Photos by E.Yu. Baraboshkin, A.Yu. Guzhikov, and V.A. Perminov. White lines show boundaries between members, numbers near lines correspond to member numbers.

onellids), lithological–mineralogical–roentgenographic, and isotopic analyses.

SECTION STRUCTURE

Outcrop 2901

Outcrop 2901 in the Dvuyakornaya Bay (45°00.060′N, 35°23.349′E) is composed of alternating dark gray clays, limestones, and siderite beds. Against the background of dominant clays, the section includes intervals enriched in limestone and siderite beds and intervals almost barren of these rocks (Figs. 2a, 2b). In this and other sections, limestones are represented by grainstones with rare relatively thicker rudstone beds. Through the entire section, limestones exhibit bioturbation features. Clays and limestones occasionally contain limonite concretions. The dip of beds varies from the northeastern in the lower part of the section to northwestern in its upper part; the dip angles largely range from 20° to 40°.

The section is characterized by the cyclic structures consist from the base upward of the following lithological units (Fig. 3):

Member 1 (samples 2901/1–2901/38) is represented by dark gray to greenish gray clays (20–170 cm) with frequent beds of light gray and pinkish limestones (grainstones) 1–30 cm thick; the thinnest beds rapidly pinch out in lateral directions. The dipping azimuth of beds varies from 20° to 68° and their dip angles range from 20° to 37°. Grainstones are composed of carbonate lithoclasts, peloids, and bioclasts of foraminifers and algae, Dasicladaceae included (Plate I, fig. 6). The bases of grainstone beds are erosional; the thickest of them are characterized by the gradational structure. The tops of grainstone beds are covered by siderite crusts (1–3 cm thick) and contain fucoids (3–6 cm below tops); locally, they demonstrate millimeter-scale ripple marks. The middle and upper parts of the member enclose rare thin (1–5 cm) siderite intercalations. Clays exhibit bioturbation structures *Phycosiphon incertum* Fisch-Ooster (Plate I, fig. 5). The ammonite assemblage from this member includes *Ptychophyllo-*

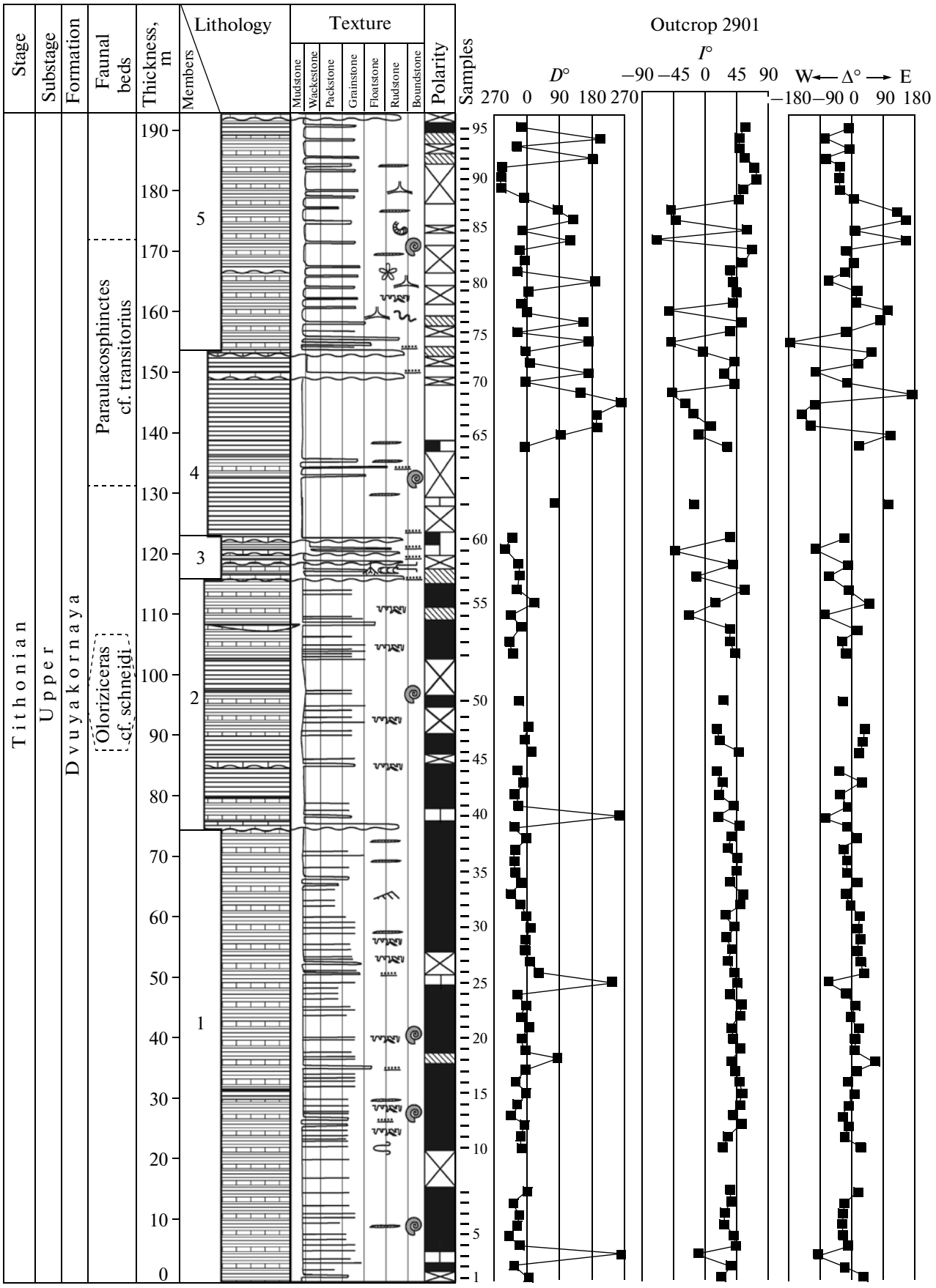
Stage
Substage
Formation
Faunal beds
Thickness, m
Members
Lithology
Texture
Mudstone
Wackestone
Packstone
Grainstone
Floatstone
Rudstone
Boundstone
Polarity
Samples
Outcrop 2901
D°
I°
Δ°
W
E
Tithonian
Upper
Dvuyakornaya
Paraulacosphinctes cf. transitorius
Oloriziceras cf. schneidi
1
2
3
4
5

Fig. 3. The results of lithological–sedimentological, paleontological and paleomagnetic investigations in Outcrop 2921 (Dvuyakornaya Bay).

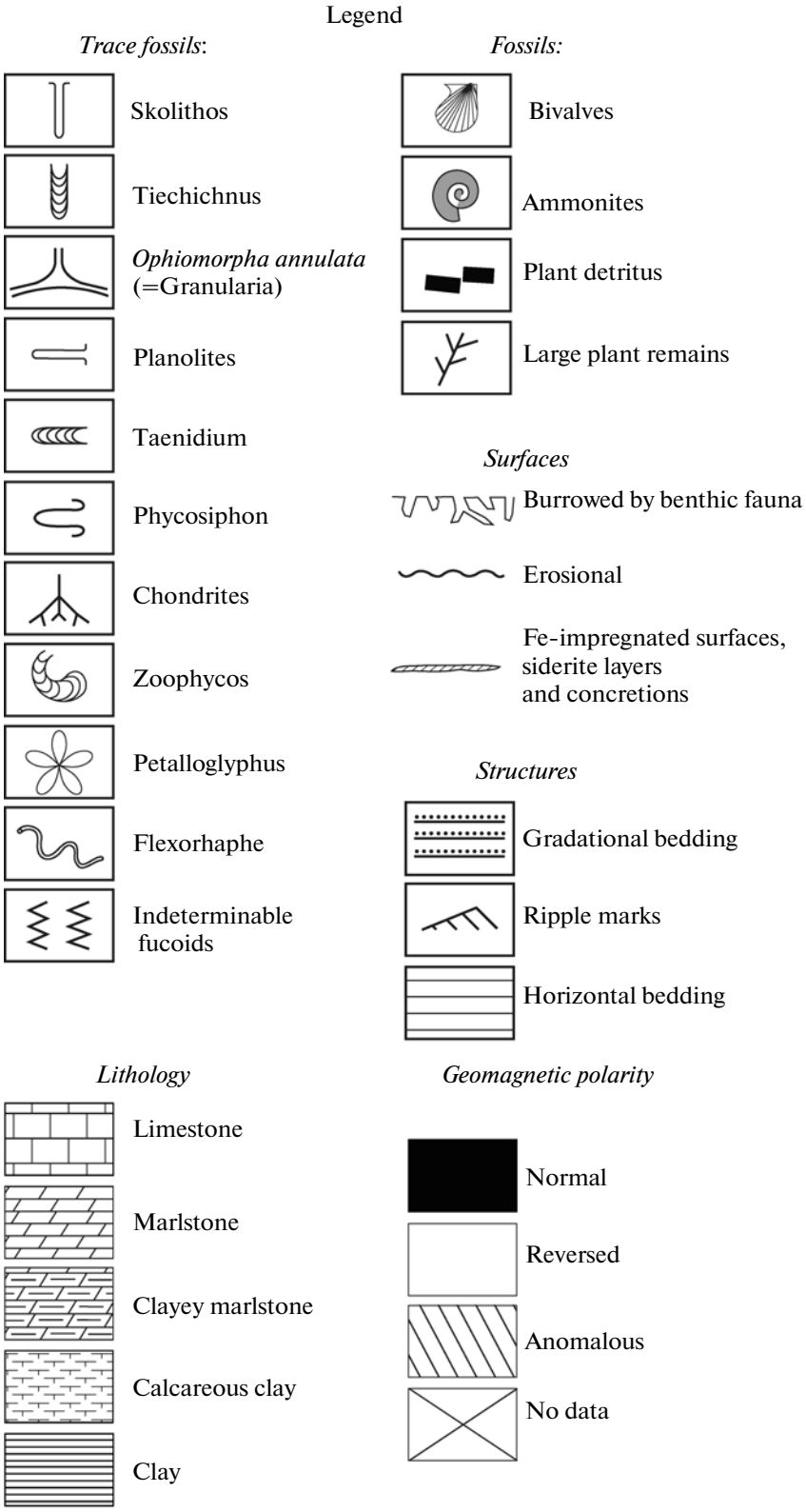

Fig. 3. (Contd.)

Plate I

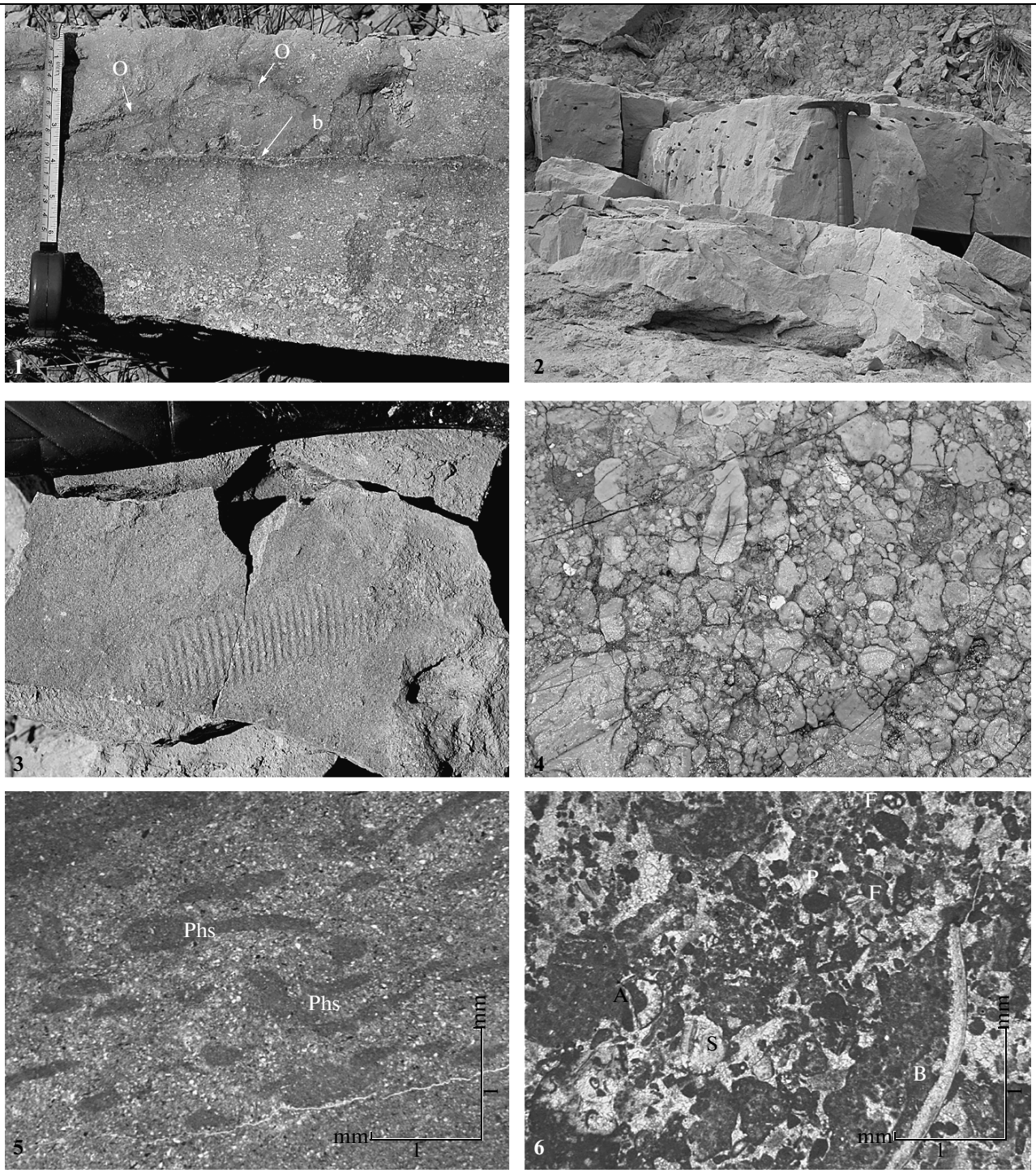

Plate I. Calciturbidite facies in examined sections: deltaic (figs. 1, 2), distributive channel (figs. 3, 4), and interchannel (figs. 5, 6). (1) doubled bed of calciturbidites with gradational bedding and erosional sideritized interface (b) and upper boundary crossed by numerous burrows of *Ophiomorpha annulata* (Ksiaz.) (O, arrows) with siderite; Dvuyakornaya Bay section, Paraulacosphinctes cf. transitorius Beds, near Sample 2901/76; (2) succession of channel turbidites separated by erosional surfaces (arrows 1 and 2) with two levels of *Ophiomorpha annulata* (Ksiaz.) burrows (O1 and O2 "holes"); the reference bed of conglomerate-like limestone in the Cape Svyatogo II'i section, lower Berriasian, Berriasella Jacobi Zone, samples 1456/1–2456/3; the hammer is 35 cm long; (3) hieroglyph of the ammonite rolling trace on the bottom; Dvuyakornaya Bay section, upper Tithonian, Oloriziceras cf. schneidi Beds, talus; (4) base of the calciturdidite (rudstone) bed; Dvuyakornaya Bay section, Paraulacosphinctes cf. transitorius Beds, above Sample 2901/59; (5) silty calcareous clay with *Phycosiphon incertum* Fischer-Ooster, 1858 (Phs); thin section 2901-12, parallel nicols; (6) grainstone with bioclasts of foraminifers (F), Dasicladaceae algae (A), and bivalves (?) (B) among rock fragments, pelloids (P); pores are filled with block calcite (S); thin section 2901-32(1), parallel nicols.

ceras sp., *Holcophylloceras* sp., *Haploceras* sp., and *Lytoceras* sp. The apparent thickness is 72.5 m.

Member 2 (samples 2901/39–2901/56) begins with a bed of pinkish rudstones with normal gradational bedding overlain by dark gray clays. The middle part of the clay section contains intercalations of light gray and pinkish grainstones 2–10 cm thick with branching burrows of *Ophiomorpha annulata* (Ksiaz.) at their tops filled with ferruginate carbonate material with the siderite matrix. This member differs from Member 1 by the lower share of grainstone beds. The member yielded ammonite form *Oloriziceras* cf. *schneidi* Tavera (Plate II, fig. 1). The thickness is 48.2 m.

Member 3 (samples 2901/57–2901/60) is composed of greenish gray clays with fucoids alternating with thick (up to 50 cm) lenticular (5–10 m long) beds of gradational grainstones–rudstones enclosing rare ooids and bioclasts and occasional intercalations of pinkish grainstones 5–10 cm thick. The grainstone beds in the middle part of the member are covered by thin siderite crusts, which lack *Ophiomorpha*. The thickness is 5.8 m.

Member 4 (samples 2901/61–2901/73) differs from the previous one in the lower share of grainstones: their thin (2–7 cm) beds occur every 1–3 m and are frequently saturated with Fe oxides, which are responsible for their brown coloration. The middle and upper parts of the member enclose grainstone–rudstone beds 20–65 cm thick with rare bioclasts. Their thickest beds exhibit superposed rhythms 5–10 cm thick with normal gradation from rud- to grainstones characterized by the successive increase of their grain size composition. Fucoids including *Ophiomorpha annulata* (Ksiaz.) are rare, occurring in the uppermost parts of grain- and rudstone beds. The member yielded finds of *Paraulacosphinctes* cf. *transitorius* (Oppel) (Plate II, figs. 2, 3) and *P.* cf. *senoides* Tavera. The thickness is 28.6 m.

Member 5 (samples 2901/74–2901/95) is characterized by frequent alternation and gray–green clays (20–100 cm), light gray to pinkish grainstones (1–10 cm) frequently covered by siderite crusts, and siderite beds. Some intervals are marked by closely spaced siderite beds and grainstone intercalations with siderite crusts. Toward the upper part of the member, the thickness of clayey beds gradually increases up to 50–180 cm; there is also a single bed of massive rudstone 35 cm thick. The sediments are bioturbated by *Zoophycos insignis* Squin. (Plate III, fig. 2), *Petalloglyphus* isp. (?), *Flexorhaphe miocenica* (Sacco) (Plate III, fig. 3) and their uppermost interval is marked by burrows of *Ophiomorpha annulata* (Ksiaz.) (Plate I, fig. 1; Plate III, fig. 5). The thickness of the member is 37.4 m. The section is crowned with a massive limestone bed 1 m thick located 7 m above the top of Member 5 and correlated with lower massive limestone beds within Member 6 in Outcrop 2922.

Outcrop 2922

Outcrop 2922, which is located in the Dvuyakornaya Bay approximately 200 m from the previous one (45°00.235′N, 35°23.144′E), with the section duplicated in neighboring outcrops 2923 and 2924 continues the section of Outcrop 2901. Its beds dip in northern and northeastern directions at angles of 10° to 34° (Figs. 2c, 4).

Member 6 (samples 2922/1–2922/11) is composed of alternating dark greenish gray clays (50–170 cm), grainstones (2–10 cm) locally with the siderite crust, siderites (1–3 cm), and thicker grain- to rudstone beds with gradational bedding (10–60 cm), which form a packet 5 m thick in its middle part. The uppermost parts of rudstone beds are crossed by *Ophiomorpha annulata* (Ksiaz.) burrows penetrating to depths of 3–5 cm; some of them are filled with siderite. The upper part of the member contains layers formed by siderite concretions and grainstones covered by siderite crusts and a single laterally sustained grainstone–rudstone bed 30 cm thick with gradational bedding. The thickness of the member is approximately 24 m.

Member 7 (samples 2922/11–2922/23, 2923/1–2923/15, 2924/1–2924/8) is represented by alternating greenish gray clays (20–200 cm), thin brownish ferruginate grainstones (2–7 cm) with siderite crusts at the top, and siderites (1–5 cm). The clay and grainstone beds with siderite crusts contain fucoids. Slightly below the mid-member at the level of Sample 2922/13, V.V. Arkad'ev found *Neoperisphinctes* cf. *falloti* (Kilian) (Plate II, fig. 4). The thickness is 36 m.

Member 8 (samples 2922/24–2922/33) is formed by regularly alternating dark gray clays (10–120 cm), light gray and pinkish grainstones (1–8 cm), brown siderites (1–10 cm), and single rudstone (20–30 cm) beds. The basal part of the member contains several thick rudstone beds barren of siderites. Some their beds up to 10 cm thick pinch out. The thickest limestone beds exhibit normal gradational bedding. The member is characterized by an admixture of plant debris and trace fossils confined to the top parts of the beds including *Planolites* isp., *Ophiomorpha annulata* (Ksiaz.), and *Scolithos* isp. In the upper part of the member, the carbonate content in the sediments begins to gradually increase, which results in coloration changes to gray and light gray and the appearance of marlstone beds. The thickness is approximately 22 m.

Outcrops 2920 and 2921

Outcrops 2920 and 2921 are located in the Cape Feodosiya area close to the boat station in the southwestern outskirts of Feodosiya 3.7 km east–northeast of the 29222 section (45°01.273′N, 35°24.895′E) continuing the latter. Its strata gently dip at angles 6°–13° westward and northwestward (Fig. 2d). Members 9 and 10 of the 2922 section are correlated with the lower part of the 2920–2921 section. Correlation is

Plate II

Plate II. Upper Tithonian and lower Berriasian ammonites of eastern Crimea.

(1) *Oloriziceras* cf. *schneidi* Tavera; specimen 376/1, lateral view (*1*); Dvuyakornaya Bay section, upper Tithonian, Microcanthum Zone, *O.* cf. *schneidi* Beds; collection by V.V. Arkad'ev; (2, 3) *Paraulacosphinctes* cf. *transitorius* (Oppel): (2) specimen 1/382, lateral view (*1*), (3) specimen 3/382: (3a) lateral view (*1*), (3b) ventral view (*1*), (3c) the same (*2*); Dvuyakornaya Bay section, upper Tithonian, Durangites Zone, P. cf. transitorius Beds; collection by V.V. Arkad'ev; (4) *Neoperisphinctes* cf. *falloti* (Kilian), specimen 34/13220: (4a) lateral view (*1*), (4b) ventral view (*1*); Dvuyakornaya Bay section, upper Tithonian (?); collection by V.V. Arkad'ev; (5) *Delphinella* cf. *obtusenodosa* (Retowski), specimen MES MSU 111/3, lateral view; bar is equal to 1 cm; Dvuyakornaya Bay, Cape Feodosiiskii, lower Berriasian, Jacobi Zone, Grandis Subzone, base of Member 11; collection by V.K. Piskunov and S.V. Rud'ko, 2010; (6) *Pseudosubplanites* cf. *euxinus* (Retowski), specimen MES MSU 111/2: (6a) lateral view, (6b) ventral view; bar is equal to 1 cm; Dvuyakornaya Bay, Cape Feodosiiskii, lower Berriasian, Jacobi Zone, Grandis Subzone, base of Member 11; collection by V.K. Piskunov and S.V. Rud'ko, 2010; (7) *Delphinella* cf. *tresannensis* (Le Hégarat, specimen MES MSU 111/1; bar is equal to 1 cm; Dvuyakornaya Bay, Cape Feodosiiskii, lower Berriasian, Jacobi Zone, Grandis Subzone, base of the Berriasian, *Jacobi* Zone, 0.45 m below the base of Member 10; collection by R.Yu. Baraboshkin, 2010.

based on presence of the thickest rudstone bed 1.2 to 3.0 m thick ("conglomerate-like limestone," after MV. Muratov, 1937; and others) in both sections, increase of the carbonate concentrations in them, and disappearance of siderites. In the 2922 section, members 9 and 10 are poorly exposed; therefore, they are described in outcrops 2920 and 2921 (Fig. 5). The samples for the paleomagnetic analysis from the reference rudstone bed are taken in the Cape Svyatogo Il'i area (Outcrop 2927, dip azimuth of the bed 36° and dip angle 12°).

Member 9 (samples 2922/34–2922/37, 2920/1–2920/10) is represented by alternating gray carbonate grainstones (10–100 cm), light gray thin-bedded marlstones (10–70 cm), and light beige grainstones (up to 10 cm). The lower part of the member encloses a single rudstone bed covered by a siderite crust. The grainstone beds are frequently located inside marlstones or immediately underlie them. The thickest grainstone beds are characterized by normal gradation bedding. Toward the member top, the thicknesses of clay beds decrease. Clays and limestones from the middle and upper parts of the member are characterized by fucoids *Skolithos* isp., *Chondrites intricatus* (Brongn.) (Plate III, fig. 4), *Planolites* isp., *Zoophycos* isp., *Tiechichnus* isp. (?), and *Taenidium* isp. The upper part of the member contains large plant detritus and ammonite species *Neolissoceras* sp., *Ptychophylloceras* sp., and *Protetragonites* sp., while layers 0.45 m below the member top (Sample 2920/1 level) yielded *Ptychophylloceras* sp., and *Delphinella* cf. *tresannensis* Le Hégarat (Plate II, fig. 7) correlating host sediments with the Berriasian Berriasella jacobi Zone. The thickness of the member increases from west eastward from 9 to 13 m.

Member 10 (samples 2921/1–2921/3). The basal part of the member corresponds to a thick reference limestone bed that is traceable from the 2922 section to the 3920–2921 section. This bed represented by channel turbidite facies rests on underlying sediments with the erosinal surface and is composed of lithoclastic rudstones with rare ooids and bioclasts of corals and bivalves. The uppermost part of the bed to depths of 20–25 cm is saturated with burrows of crustaceans *Ophiomorpha annulata* (Ksiaz.). In the Cape Svyatogo Il'i section, the thickness of this bed exceeds 3 m on account of repeated channel rhythms that include rud- to grainstones with gradational bedding and erosional surface disturbed by *Ophiomorpha* burrows (Plate I, fig. 2). There are three such cycles: the lower cycle is composed of breccias with gradational bedding and the upper one is formed by coarse-grained grainstones. In this bed, Arkad'ev (2003) found *Haploceras* sp. It is overlain by a sequence of alternating gray carbonate clays (30–150 cm), light beige grain- to rudstones with gradational bedding (3–70 cm), and light gray marlstones (up to 10 cm). The transition of clays to marlstones is frequently gradual and they enclose lenses of grainstones up to 7 cm thick. The upper part of the member contains beds of light beige limestones represented by grain- and rudstones from 20 to 130 cm thick. The sediments 5 m above the member base yielded ammonites *Berriasella chomeracensis* (Touc.), *Fauriella* cf. *floquinensis* Le Heg., *Ptycophylloceras* cf. *semisulcatum* (d'Orb.), and *Haploceras* sp. (Arkad'ev, 2003). The thickness is 7.8 m.

Member 11 (samples 2921/4–2921/10) is characterized by almost complete lack of limestones being represented by alternating gray clays (0–300 cm) and light gray marlstones (30–50 cm). Only single level in middle part of the member is marked by grainstone lenses (up to 5 cm thick) occurring inside a marlstone bed. The carbonate content increases from the base of clay beds toward the top of marlstone beds. Some levels contain rare large plant detritus, limonite concretions, and fucoids. In 2010, V.K. Piskunov and S.V. Rud'ko found at 7.8 m above the member base (Sample 2921/4 level) ammonites *Pseudosubplanites* cf. *euxinus* (Ret.), *Delphinella* cf. *obtusenodosa* (Ret.) (Plate II, fig. 5) and *D.* sp. indet., which allow the lower boundary of the Pseudosubplaites grandis Subzone to be placed at the base of Member 11. The thickness is 16 m.

Member 12 (samples 2921/11–2921/13) (member of the "Feodosiya Marlstone") differs from the previous one by development of thicker (30–80 cm) marlstone and frequent grainstone beds and lenses (up to 5 cm thick) among clays and marlstones. The rocks are marked by single fucoids. The apparent thickness is 4 m.

In 2004, members 10–12 in the Cape Svyatogo Il'i (Fig. 6) were sampled for paleomagnetic studies (Yampol'skaya et al., 2006, 2009): samples 2456/1–2456/15

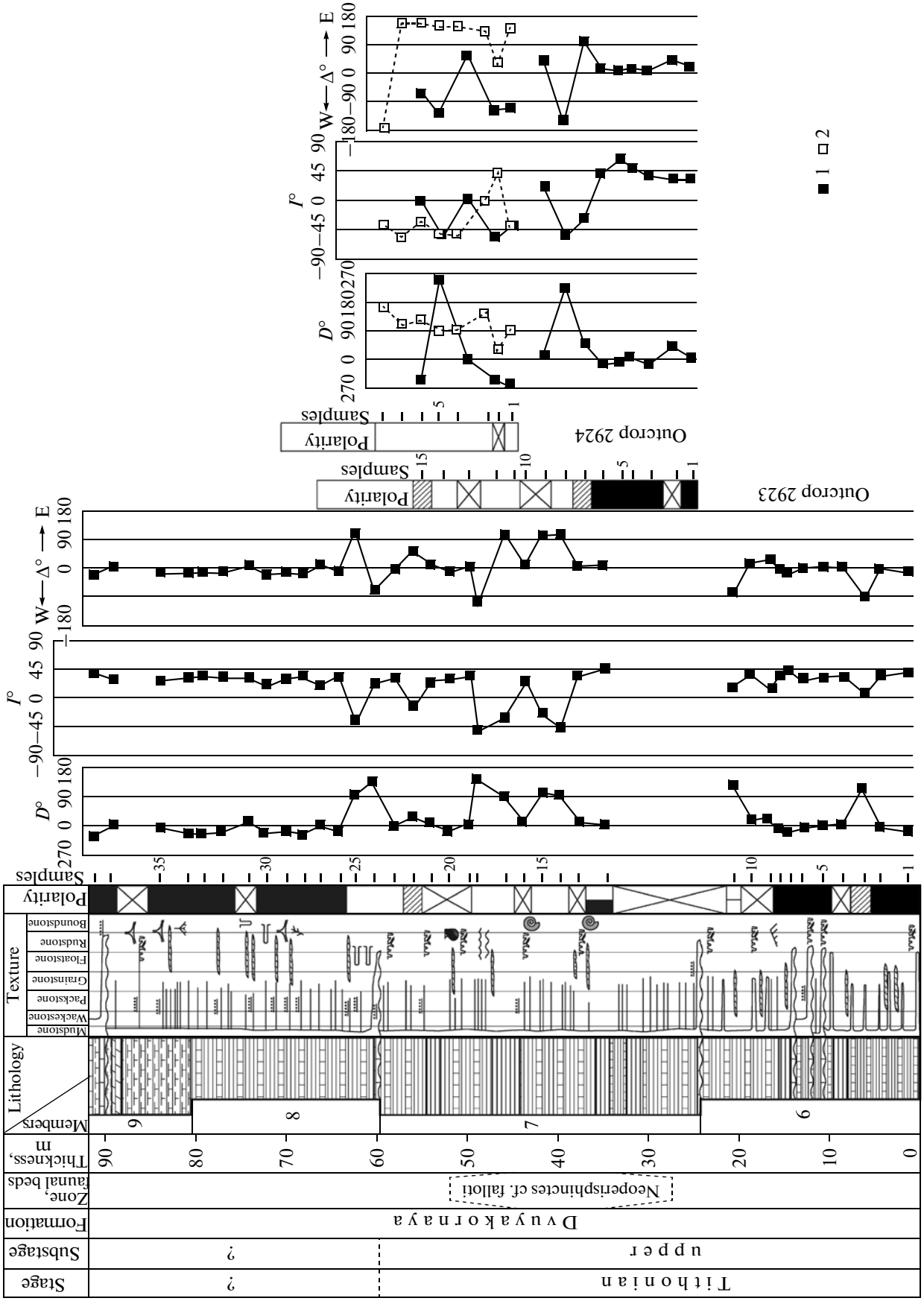

Fig. 4. The results of lithological–sedimentological, paleontological and paleomagnetic investigations in outcrops 2922–2924 (Dvuyakornaya Bay). Symbols: (1, 2) data on outcrops 2923 and 2924, respectively. For other symbols, see Fig. 3.

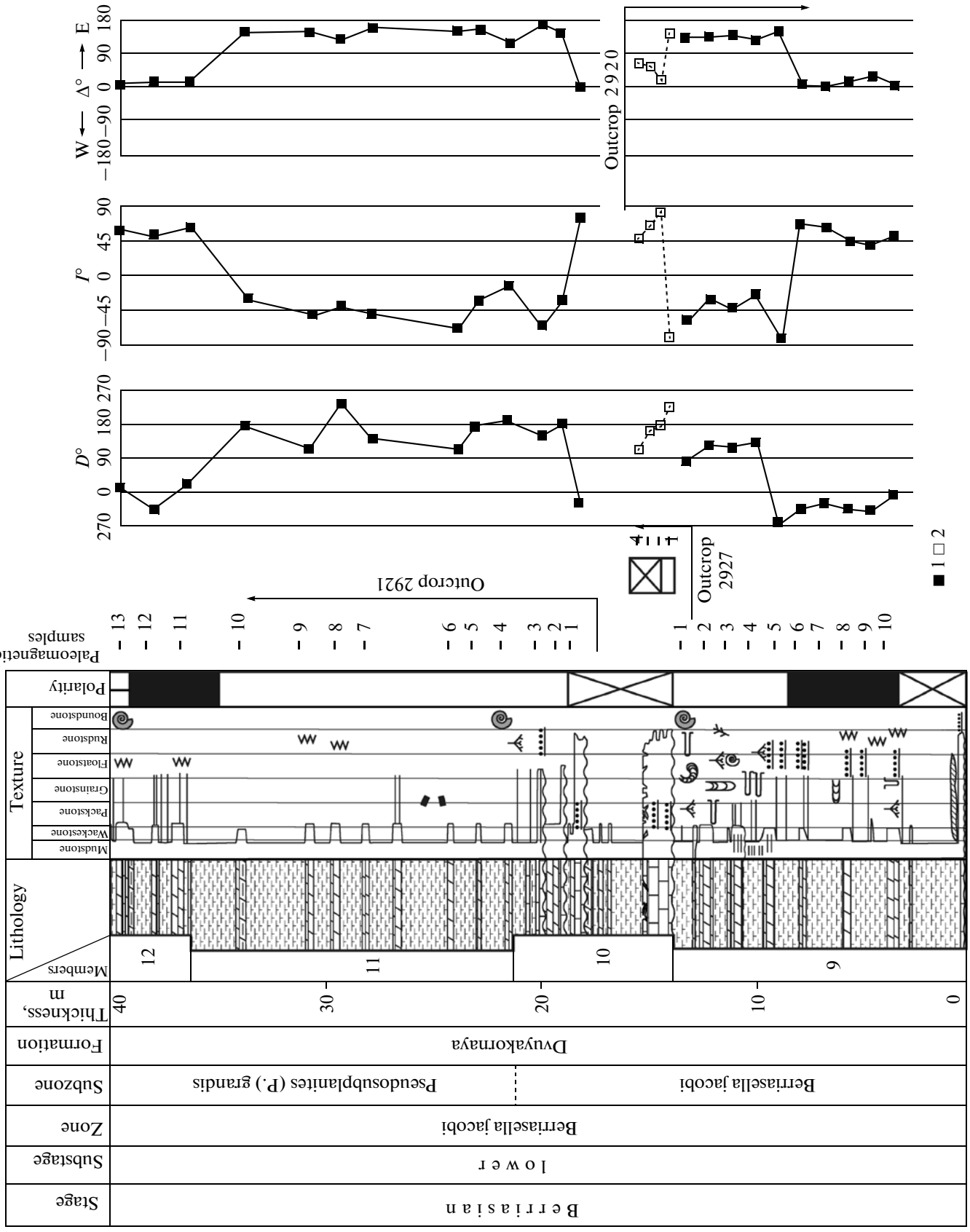

Fig. 5. The results of lithological–sedimentological, paleontological and paleomagnetic investigations in outcrops 2920, 2921 (Cape Feodosiiskii), and 2927 (Cape Svyatogo Il'i).

Symbols: (1, 2) data on outcrops 2920–2921 and 2927, respectively. For other symbols, see Fig. 3.

Plate III

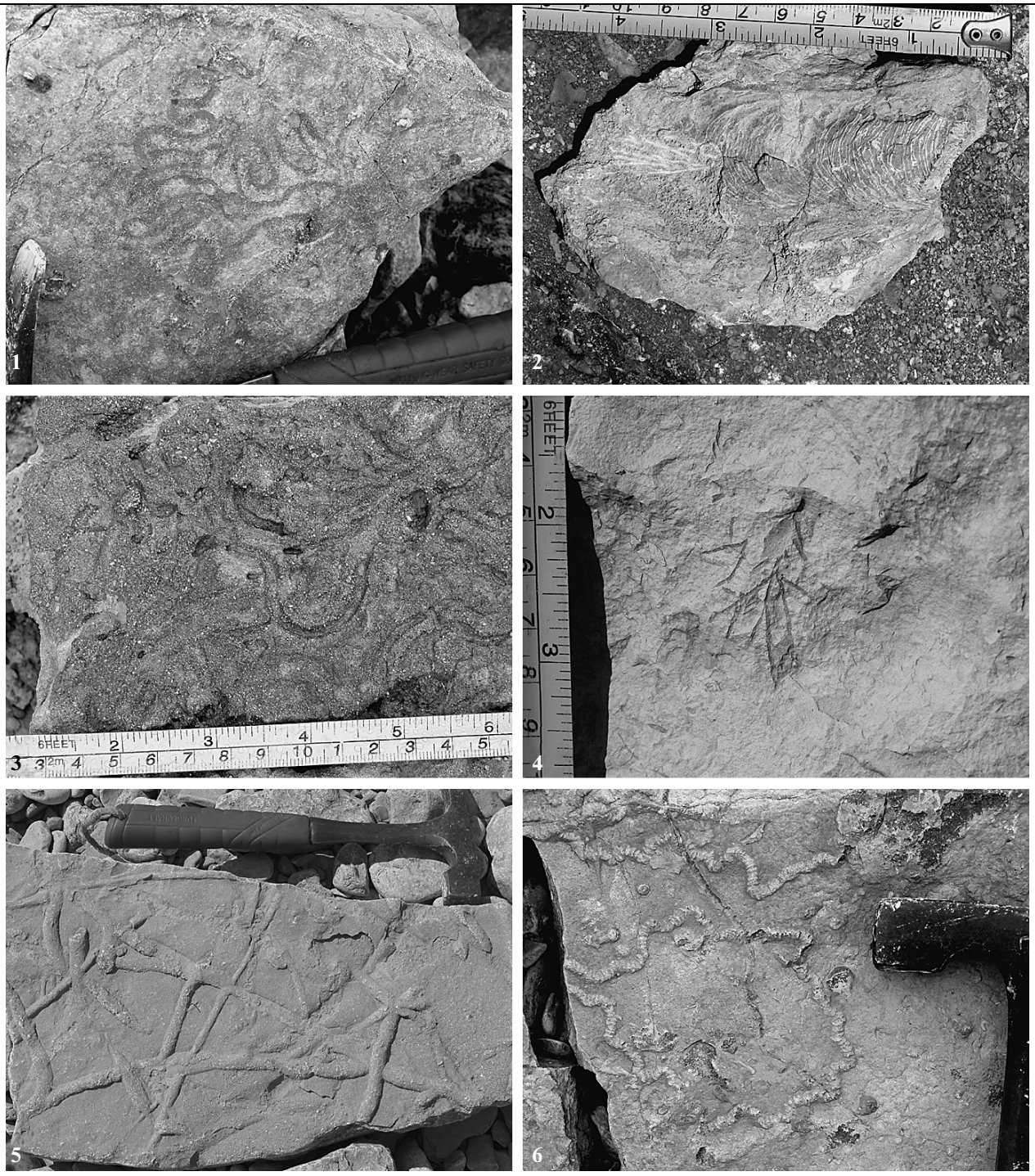

Plate III. Some trace fossils from the examined sections.

(1) *Cosmorhaphe lobata* Seilacher, 1977; Cape Svyatogo Il'i section, lower Berriasian, Berriasella jacobi Zone, talus; (2) *Zoophycos insignis* Squinabol, 1890; Dvuyakornaya Bay section, upper Tithonian, Paraulacosphinctes cf. transitorius Beds, near Sample 2901/78; (3) *Flexorhaphe miocenica* (Sacco); Dvuyakornaya Bay section, upper Tithonian, Paraulacosphinctes cf. transitorius Beds, near Sample 2901/78; (4) *Chondrites intricatus* (Brongniart, 1823); Cape Feodosiiskii section, lower Berriasian, Grandis Subzone, talus; (5) *Ophiomorpha annulata* (Ksiazkiewicz, 1977); Dvuyakornaya Bay section, upper Tithonian, Paraulacosphinctes cf. transitorius Beds, near Sample 2901/76; (6) *Nereites missouriensis* (Weller, 1899); Cape Feodosiiskii section, lower Berriasian, Grandis Subzone, talus.

from Member 10, samples 2456/16–2456/45 from Member 11, and samples 2456/46–2456/56 from Member 12. The last member contains the diverse ammonite assemblage of the Grandis Subzone: *Pseudosubplanites grandis* (Maz.), *P. ponticus* (Ret.), *P. lorioli* (Zitt.), *P. combesi* Le Hog., *P. subrichteri* (Ret.), *Berriasella berthei* (Touc.), *Delphinella subchaperi* (Ret.), *D. crimense* (Burckh.), *D. obtusenodosa* (Ret.), *D. tresannensis* Le Hog., *D. janus* (Ret.), *D. pectinata* Arkad. et Bogd., *Retkowskiceras* sp., *Tirnovella* sp. (Arkad'ev et al., 2008).

DEPOSITIONAL ENVIRONMENTS

According to Baraboshkin (2005), in the terminal Tithonian–initial Berriasian, the area in question represented the steep slope of a stepped ramp, which accumulated the thick hemipelagic and gravitational sediments considered in this work. They include several genetic types:

(1) Calciturbidites with main channel, distributive channel, and interchannel facies.

Channel turbidites (Plate I, figs. 1, 2) are represented by thickest (40–300 cm) rudstone and grainstone beds of lenticular shapes and variable thicknesses. Their section consists of several channel cycles that include the erosional surface and sediments with gradational bedding, the upper part of which is usually disturbed by *Ophiomorpha annulata* (Ksiaz.) (=*Granularia*) burrows. The most remarkable example of such facies is a reference bed inside Member 10 at the base of the Berriasian section (Plate I, fig. 2). The low proportion of channel facies, and the occurrence of several levels bioturbated by *Ophiomorpha* in them imply relatively uncommon turbidity flows, deficiency of coarse-grained material, and a dominant role of hemipelagic sedimentation.

Facies of distributive channels characterized by the lower thickness is composed of limestones with gradational bedding and textures ranging from rudstones to coarse-grained grainstones (Plate I, fig. 4). The erosional base is usually flat, rarely with hieroglyphs, and, occasionally, with ammonite rolling traces (Plate I, fig. 3). The upper surface is locally disturbed by *Ophiomorpha annulata* (Ksiaz.) burrows, although the section structure reflects a single-event turbidity flow.

Interchannel facies are formed by alternating calcareous hemipelagic clays and grainstones (Plate I, figs. 5, 6). The thicknesses of grainstone beds vary from a few centimeters to millimeters. They exhibit normal gradation with occasional millimeter-scale cross-bedded structure and their tops are locally disturbed by *Ophiomorpha* burrows. The intervals of frequently alternating clays and grainstones may be interpreted as representing facies of near-cannel bars and intervals with their rare alternation, as interchannel facies proper.

The coarse-grained composition of these sediments and lack of a complete Bouma succession make all the sediments under consideration similar to coarse-grained high-density turbidites. Clays separating turbidite beds demonstrate horizontal bedding, although they are frequently bioturbated (Plate I, fig. 5), which indicates their relatively shallow depositional environments. The sediments frequently exhibit deformations in the form of small folds and detachments, the nature of which (syngenetic or superposed tectonic) remains unclear.

(2) Hemipelagites are largely represented by frequently bioturbated clays and slightly calcareous clays in the Jurassic part of the section and by calcareous clays and marlstones both laminated and bioturbated in its Cretaceous interval.

The peculiar feature of these sediments is the increase in the carbonate contents upward the section against a background of channel turbidites occurring in the lower part of the section and their almost complete lack at higher levels (members 11 and 12). It seems more reasonable to identify "distal turbidites" from Member 12 as hemiturbidites (Stow and Wetzel, 1990). Such a transition is most likely explained by cessation of turbitite sedimentation and onset of shallow-water pelagic sediment deposition, which was accompanied by a decrease in sedimentation rates and partly supported by higher concentrations of carbonate nannofossils (Matveev, 2009). No significant hiatuses could appear in such depositional environments.

Thus, marly sediments were likely deposited in shallower and/or warmer settings under higher productivity compared with background calcareous clays, which is confirmed by maximal concentrations of nannofossils in them (Matveev, 1989).

The analysis of trace fossils revealed that their Jurassic and Cretaceous assemblages are different. The Tithonian turbidite sediments contain burrows of the worms *Phycosiphon incertum* Fisch-Ooster (Plate I, fig. 5), *Zoophycos insignis* Squinabol (Table III, fig. 2), *Flexorhaphe miocenica* (Sacco) (Plate III, fig. 3), *Chondrites* isp., *Planolites* isp., *Petalloglyphus* isp. (?), *Taenidium* isp. and crustaceans *Ophiomorpha annulata* (Ksiaz.). The last structures are frequent occurring at both bases of turbidite beds (Plate III, fig. 5) and tops of channel turbidites (Plate I, fig. 1) and marking pre- and postturbidity events (Braboshkin and Yanin, 2011).

The assemblage of Berriasian trace fossils is more diverse and includes burrows of worms *Nereites missouriensis* (Weller) (Plate III, fig. 6), *Chondrites intricatus* (Brongniart) (Plate III, fig. 4), *Ch.* isp, *Planolites* isp., *Rhizocorallium* isp., *Glockeria parvula* Ksiaz., traces of Coelenterata resting places (*Berguaeria perata* Prantl), farmer structures *Cosmorhaphe lobata* Seilacher (Plate III, fig. 1), and crustacean burrows *Ophiomorpha annulata* (Ksiaz.). *Ophiomorpha* burrows are usually confined to the basal part of the section and associate with channel turbidites (Plate I, fig. 2). In addition, these sediments contain farmer structures *Paleodictyon* isp., worm burrows *Taenidium* isp., *Peta-*

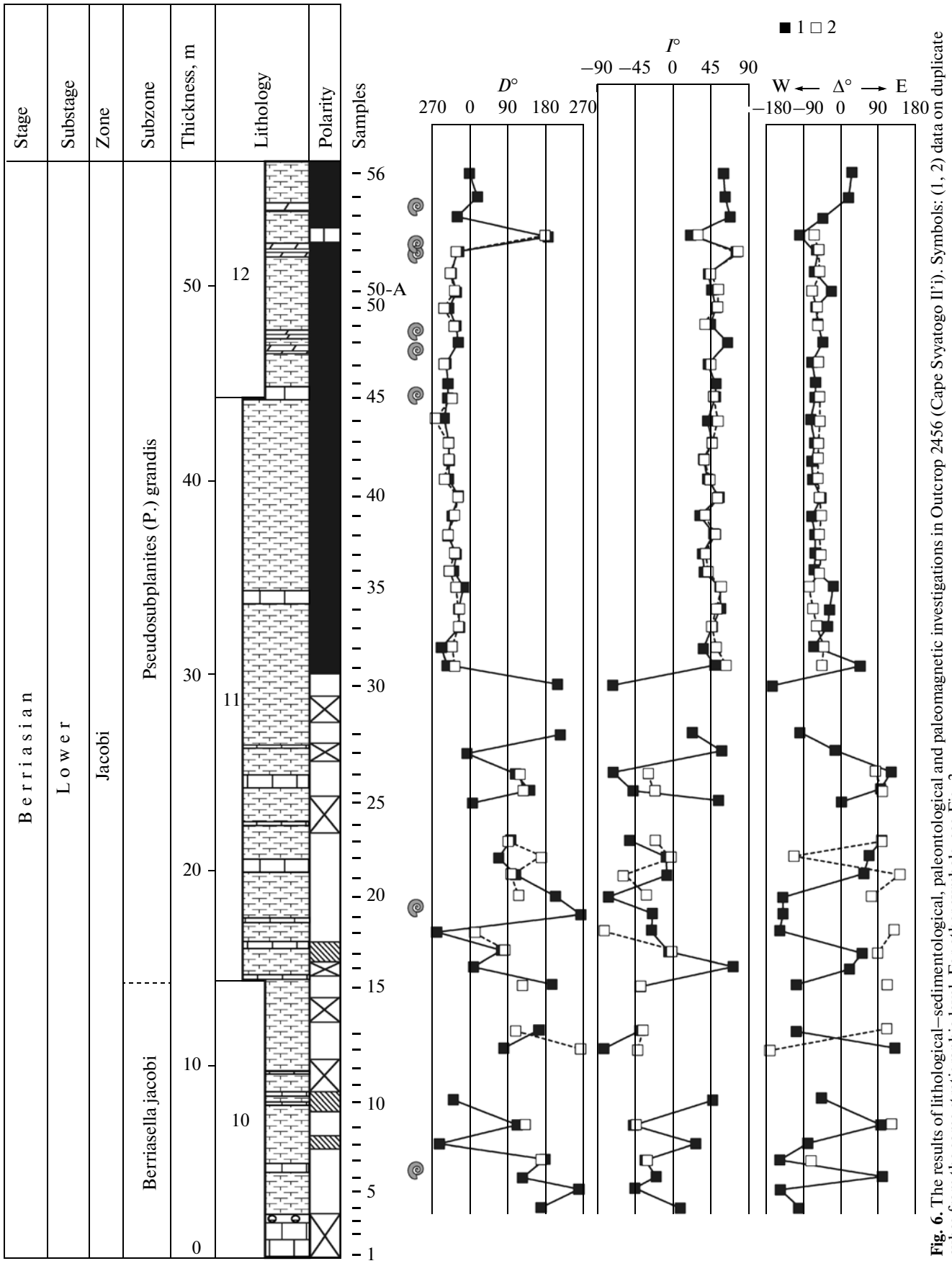

Fig. 6. The results of lithological–sedimentological, paleontological and paleomagnetic investigations in Outcrop 2456 (Cape Svyatogo Il'i). Symbols: (1, 2) data on duplicate cubes from the same stratigraphic level. For other symbols, see Fig. 3.

loglyphus isp., *Stelloglyphus* isp., *Haentzschelinia* isp., *Spirorhaphe* isp., and *Zoophycos* isp. (Yanin and Baraboshkin, 2010; Baraboshkin and Yanin, 2011).

Both assemblages characterize the *Nereites* ichnofacies peculiar of the basin slope base and bottom settings each their different parts: relatively deeper (Jurassic) and shallower (Cretaceous) (Baraboshkin and Yanin, 2011). The latter is evident from the occurrence of the shallower *Gruziana (Bergaueria)* ichnofacies in the Berriasian interval. It is noteworthy that the *Zoophycos* ichnofacies is indefinable.

Thus, the examined section reflects two stages in the ramp development. The first of them corresponds to the Late Jurassic (members 1–8), when turbidites were accumulating against a background of basin bottom subsidence and intense hemipelagic sedimentation. The second stage coincides with the terminal Tithonian and early Berriasian (members 9–12), when turbidite deposition practically ceased being replaced by less intense hemipelagic sedimentation. Despite the difference in sedimentation rates, they remained relatively high during both stages and no presumable regional hiatuses are registered in the section. This provides grounds for the conclusion that the stratigraphic record of the Jurassic–Cretaceous boundary interval is sufficiently complete.

BIOSTRATIGRAPHY

The study of the Dvuyakornaya Formation section revealed upper Tithonian ammonite remains at different stratigraphic levels: *Oloriziceras* cf. *schneidi* Tavera (Plate II, fig. 1), *Paraulacosphinctes* cf. *transitorius* (Oppel) (Plate II, figs. 2, 3), *P.* cf. *senoides* Tavera, *Neoperisphinctes* cf. *falloti* (Kilian) (Plate II, fig. 4) (Arkad'ev, 2004, 2011; Arkad'ev et al., 2006, 2010; Arkad'ev and Rogov, 2006). In the continuous upper Tithonian–Berriasian section of the Feodosiya area, the barren interval between beds with upper Tithonian and Berriasian ammonites is approximately 40 m thick. The distribution of the genus *Oloriziceras* is limited by the Simplisphinctes Subzone of the Microcanthum Zone (Tavera, 1985), whereas *P. transitorius* is an index species of the synonymous zone in the Mediterranean region (Geyssant, 1997; Hoedemaeker and Rawson, 2000). Correspondingly, V.V. Arkad'ev defined in the Feodosiya section the Oloriziceras cf. schneidi Beds (Member 2) and Paraulacosphinctes cf. transitorus Beds (Member 4). The first beds are included into the upper Tithonian Microcanthum Zone and others, with account for the new magnetostratigraphic data (Arkad'ev et al., 2010), into the Durangites Zone. The genus *Neoperisphinctes* is known from the *Transitorius* Subzone of the upper Tithonian Durangites Zone of Spain (Oloriz and Tavera, 1982; Tavera, 1985). In the Puerto Escano section, it is recorded in the upper part of the Durangites Zone (Tavera et al., 1994). It should, however, be noted that the Crimean species *N.* cf. *falloti* is represented by a single incomplete specimen, which casts doubt upon its identification. Therefore, the conclusion on the late Tithonian age of N. cf. falloti Beds is preliminary.

In 2010, the Berriasian ammonite species *Ptychophylloceras* sp. and *Delphinella* cf. *tresannensis* Le Hégarat (Plate II, fig. 7), which characterize the Jacobi Zone, were found at the top of Member 9 in the Feodosiya section below the 2–3-m-thick reference limestone bed. The higher layers yielded ammonite assemblages which indicate the presence of two, Jacobi and Grandis, subzones of the Jacobi Zone in this section. Owing to new finds of Berriasian ammonites, the base of the Berriasian Stage there is placed 0.45 m below the top of Member 9, while the lower boundary of the Grandis Zone is drawn at the base of Member 11 (Figs. 5, 6, Table 1).

The specimen of *Neoperisphinctes* cf. *falloti* (Kilian) described in this article is stored at the Central Research Geological–Prospecting Museum, St. Petersburg (collection 13220) and specimens of *Pseudosubplanites* cf. *euxinus* (Ret.) and *Delphinella* cf. *tresannensis* Le Hég., in the Museum of Earth Sciences of the Moscow State University (MES MGU), Moscow (collection 111). Other specimens of upper Tithonian ammonites pictured here are stored at the Paleontological–Stratigraphic Museum of the Chair of Dynamic and Historical Geology in the St. Petersburg State University (collections 376 and 382).

TAXONOMIC DESCRIPTION

Suprafamily Perisphictaceae Steinmann, 1890

Family Perisphinctidae Steinmann, 1890

Genus *Neoperisphinctes* Tavera, 1985

Type species. *Perisphinctes falloti* Kilian, 1889; Tithonian of southeastern France.

***Neoperisphinctes* cf. *falloti* (Kilian)**

Plate II, fig. 4

Shape. A single deformed specimen is characterized by the discoid evolute shell with gradually increasing whorls and slightly convex lateral and flattened ventral sides. Lateral sides join the ventral one through the distinct bend, where ribs become slightly thicker. Umbilicus is wide, stepped, with a steep wall.

Ornamentation. Lateral sides are covered by doubled straight ribs that begin on the umbilical side. Ribs bifurcate into identical branches approximately at two thirds of the whorl slightly increasing in the ventral–lateral bend areas and passing without bending and weakening through the ventral side.

Size (mm) and ratios (%).

Specimen number	D	H	W	D_u	H/D	W/D	D_u/D
34/13220	64.0?	21.8	12.0?	31.0	34?	19?	49?

Comparison and remarks. Our specimen is close to *Neoperisphinctes falloti* (Tavera, 1985, plate 16, fig. 10) from the upper Tithonian of Spain. The species under consideration differs from *N. nexus* Tavera by the more flattened ventral side. At the same time, very rare ribs on inner whorls make our specimen different from known *Neoperisphinctes* species. This ammonite species is also close to representatives of the genus *Durangites*, which is characterized by the slightly wider geographic distribution (Mexico, Cuba, Spain, France, Tunisia, Bulgaria, India, and other regions) being known from the both upper Tithonian and basal Berriasian.

Material. Single specimen from Eastern Crimea (outskirts of the Ordzhonikidze Settlement, Dvuyakornaya Bay), upper Tithonian (?), middle part of Member 7, collection by V.V. Arkad'ev, 2010.

Suprafamily Olcostephanaceae Pavlov, 1982
Family Neocomitidae Salfeld, 1921
Genus *Pseudosubplanites* Le Hégarat, 1971
Pseudosubplanites cf. *euxinus* (Retowski)

Plate II, fig. 6

Shape. Shell is small (D = 30 mm), evolute. Umbilicus is wide (D_u = 11 mm), shallow; the umbilical side is moderately narrow grading into sides. The transverse section is rounded–rectangular, elongated in height (H = 10 mm), and slightly widened in the middle part (W = 5 mm).

Ornamentation. Ribs are closely spaced, sigmoidal, bifurcating, rarely fasciculate or solitary; one bidichotome rib is observable. Bifurcating ribs ramify in the upper third of the lateral side; in adult shells the branching point is located slightly lower. Fasciculate and bidichotome ribs first ramify slightly above the umbilical bent and, then, in the upper third of the lateral side. The number of ribs in the half-whorl: 20 at the umbilical bent and 37 at the ventral bent. All the ribs cross the ventral side retaining their heights. Each whorl is marked by five vague narrow strictures.

Comparison and remarks. Our specimen differs from the lectotype of *P. euxinius* (Retowski, 1893, p. 254, plate X, figs. 6, 7) proposed in (Mazenot, 1939, p. 125), by development of a single bidichotome rib. Specimens attributed to *P. euxinus* (Le Hégarat, 1971) are characterized by more involute shells with the high section and high rib bifurcation point and belong, in our opinion, to the different species. Bogdanova and Arkad'ev (2005) consider the species *P. euxinus* as a synonym of *P. lorioli*. According to E.Yu. Baraboshkin, *Pseudosubplanites lorioli* (Zittel) differs from *P. euxinus* by more regular bifurcating ribs, absence or rare development of fasciculate ribs, and wider transverse section.

Material. One slightly deformed specimen stored in the Museum of Earth Sciences of the Moscow State University, Sample 111/2 from the Cape Feodosiiskii section, lower Berriasian, Berriasella jacobi Zone, Pseudosubplanites grandis Subzone, Member 11, collection by V.K. Piskunov and S.V. Rud'ko, 2010.

Genus *Delphinella* Le Hégarat, 1971
Delphinella cf. *tresannensis* Le Hégarat

Plate III, fig. 7

Shape. Shell is small (D = 27 mm), flattened, semiinvolute, with high (H = 11 mm) narrow whorls. Umbilicus is moderately narrow (D_u = 5.5 mm), shallow; the umbilical wall is narrow, steep. The ventral side is inaccessible for observation.

Ornamentation. Ribs are thin, closely spaced, bended, bipartite, intercalating and, less commonly, tripartite or single. Bipartite ribs ramify in the lower third of the lateral side. Tripartite ribs ramify first slightly above the umbilical bent and then in the upper third of the lateral side. The main rib may be both first and last in the fascicule. The number of ribs in the half-whorl is 28 at the umbilical bend and 60 near the ventral bend.

Comparison and remarks. Our specimen is similar to inner whorls of the *Delphinella tresannensis* Le Hégarat specimen pictured in (Arkad'ev and Bogdanova, 2005, plate V, fig. 5). *D. tresannensis* is known from the Jacobi Zone of Crimea (Grandis Subzone), southeastern France, and Spain.

Material. One juvenile specimen compressed along the plane of symmetry is stored in the Museum of Earth Sciences of the Moscow State University, Sample 111/1 from the Cape Feodosiiskii section, basal Berriasian, Berriasella jacobi Zone, 0.45 m below the base of Member 10 (reference bed of a thick channel turbidite sequence), collection by E.Yu. Baraboshkin, 2010.

MAGNETOSTRATIGRAPHY

Petromagnetic and magnetic–mineralogical investigations were conducted to assess the appropriateness of samples for paleomagnetic measurements and obtain additional information on the composition of examined sections (or more exactly, on the distribution of the ferromagnetic fraction in them). These investigations included the analysis of magnetic susceptibility (K) and its anisotropy, measurements of natural remanent magnetization ($\mathbf{J_n}$), experiments of magnetic saturation with subsequent measurements of remanent saturation magnetization ($\mathbf{J_{rs}}$) and remanent coercive force (H_{cr}), and differentiated thermomagnetic analysis (DTMA). The magnetic susceptibility was measured at the MFK-1FB equipment (Kappabridge) and remanent magnetization, at the JR-6 spinner magnetometer; the thermal analyzer of fractions (TAF-2) or "magnetic weights" was used.

The presence of magnetite or relative minerals is determined based on rapid magnetization decrease at temperatures of 530–570°C, which are close to the Fe_3O_4 Curie point (578°C) and typical of its finely dispersed fractions, in the DTMA curves (Fig. 7a). Its occurrence is also indirectly confirmed by relatively low values of saturation fields (100–200 mT) and remanent coercive force (20–30 mT) characteristic of the soft magnetic phase (Figs. 7b, 7c).

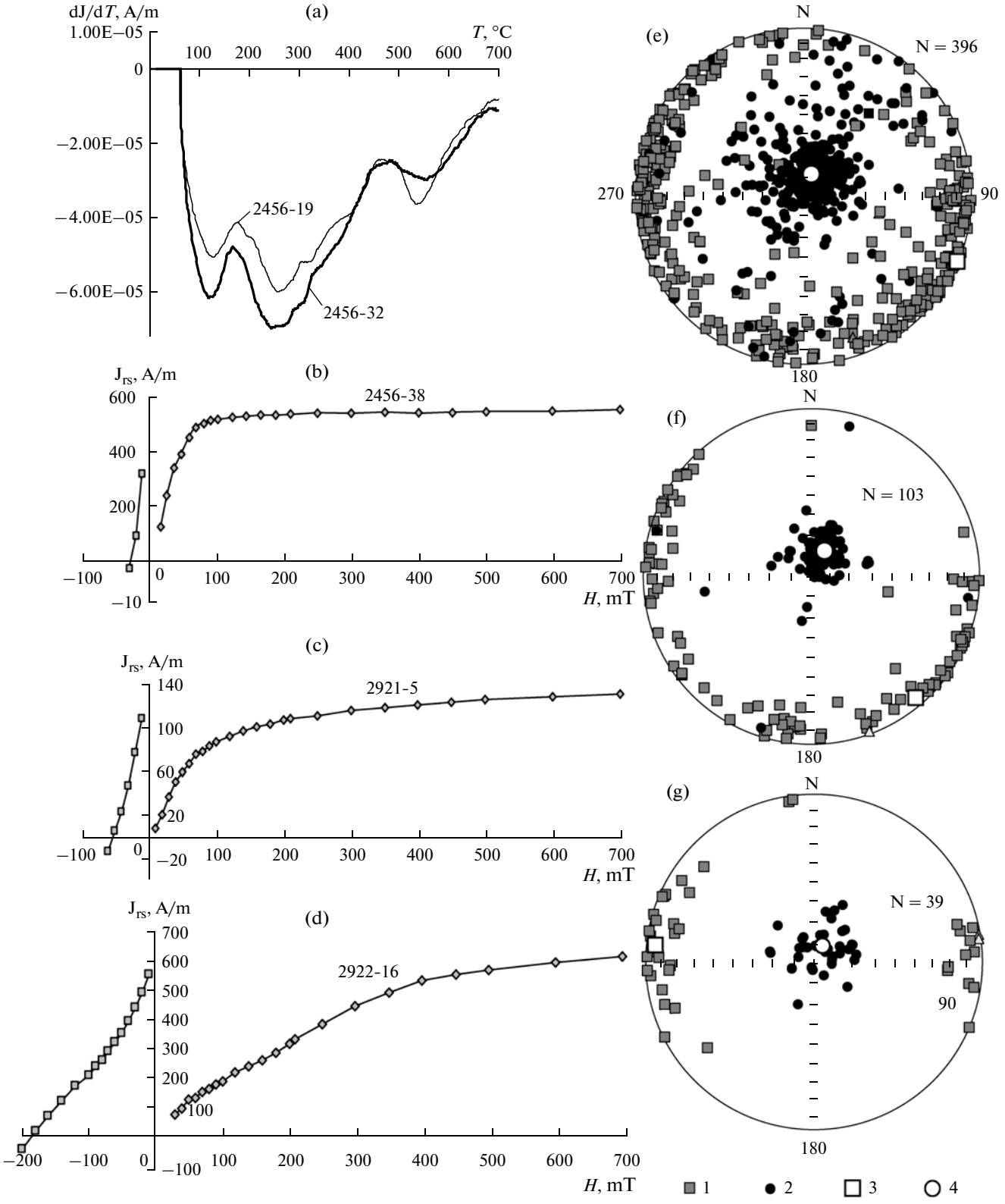

Fig. 7. The results of the magnetic–mineralogical analysis and analysis of the magnetic structure.

(a) DTMA curves (first derivatives from curves of the thermomagnetic analysis); (b–d) magnetic saturation curves; (e–g) distributions of directions of magnetic susceptibility anisotropy ellipsoid axes (in the stratigraphic coordinate system) for all samples (e), for samples from outcrops 2456, 2920, and 2921 (f) and for clays from Outcrop 2901 (g).

(1, 2) long (*K1*) and short (*K3*) axes of magnetic susceptibility anisotropy ellipsoids, respectively; (3, 4) average *K1* and *K3* values, respectively.

At the same time, the DTMA data reveal practically for all the examined samples additional minimums approximately at 120 and 250°C that disappear under repeated heating, while magnetic saturation plots demonstrate very gradual insignificant magnetization growth up to fields of 720 mT even in softest magnetic samples with H_{cr} of <30 mT (Fig. 7b). In some samples, H_{cr} increases up to 50–60 mT and the $\mathbf{J_{rs}}$ growth on the gentle branch of the curve becomes more notable (Fig. 7c). Only four samples from the entire section appeared to be magnetically hard: magnetic saturation in them was never reached in fields of 500 mT and higher, while the coercive force was as high as 200–350 mT (Figs. 7d, 8).

Such a behavior of the DTMA curves and magnetic saturation are readily explained by partial maghemitization and variable martitization of the surface of magnetite, a main magnetization carrier. Maghemite, a product of single-phase Fe_3O_4 oxidation is probably reflected by a bent at ~250°C in DMTA curves, while the inflection at ~120°C combined with the increase in the magnetic hardness implies development of hydroxides dehydrated in the variable degree: up to hematite (martite).

The anisotropy of magnetic susceptibility in examined samples demonstrates a distinct regularity: average values of minimal anisotropy axes are significantly displaced from the center of stereoprojection and their distribution is confined to arches of great circles that are inconsistent with stereogram edges (Fig. 7a–7g). These data suggest that initial sediments were deposited on the inclinded surface and confirm the abovementioned conclusion that they accumulated on the ramp slope inferred from the sedimentological analysis. The differentiated analysis of the magnetic structure carried out for separate intervals of the composite section and lithological varieties reveals additional regularities. For example, the anisotropy K in the uppermost part of the section is poorly expressed (Fig. 7f). On the contrary, clays from its basal part demonstrate the strong anisotropy of long axes of magnetic ellipsoids in the W–E direction (Fig. 7g), while magnetic structure of limestones from the same interval is chaotic. Based on these data and other peculiarities of the anisotropy K in the section under consideration, it was previously assumed that clays acquired plastic deformation on the steep slope at the stage of unconsolidated sediments (Bagaeva et al., 2010).

The examined rocks are characterized by low to moderate natural magnetization, which generally increases upward the section: K (0.4–100.7 × 10^{-5} SI units and $\mathbf{J_n}$ (0.06–62.9 × 10^{-3} A/m (Fig. 8). The minimal magnetic susceptibility (<10 × 10^{-5} SI units) is characteristic of limestones from the lower part of the section. The plot illustrating the $K/\mathbf{J_{rs}}$ parameter reflecting the average size of ferromagnetic grains in the rock is very expressive: its maximal values corresponding to the maximal average size of ferromagnetic particles are characteristic of the uppermost part of the section (members 10–12) (Fig. 8), which is, probably, explained by the intensified terrigenous influx in the Berriasian. This interval is underlain by members 7–9 characterized by anomalously high H_{cr} values (200–350 mT) (Fig. 8). It may be assumed that they reflect the admixture of allothigenic magnetite grains, which arrived at the basin being strongly martitized.

In the context of the $\mathbf{J_n}$ nature discussion, of particular interest is information on the Q factor (Koenigsberger's parameter representing a ratio between remanent and inductive magnetization). The entire section, except for its 10-m-thick interval in Member 11 is characterized by $Q \leq 1$ (mostly $Q \ll 1$) (Fig. 8), which is typical of orientation magnetization. For the uppermost part of Member 11, where Q varies from 1 to 1.49 and the size of ferromagnetic grains is minimal (judging from the $K/\mathbf{J_{rs}}$ plot in Fig. 8), the chemical nature of magnetization cannot be excluded.

Paleomagnetic measurements. For the paleomagnetic analysis aimed at obtaining magnetic polarity characteristics, each of 240 oriented samples taken from different stratigraphic levels (Fig. 3–6) was split into 3–4 cubes with ribs 20 mm long. The laboratory paleomagnetic study consisted in measurements of natural remanent magnetization ($\mathbf{J_n}$) of samples at the JR-6 spinner magnetometer after several magnetic cleaning operations by alternating current (mostly up to 50 mT with the step of 5 mT) at the LDA-3 AF equipment and heating at temperatures of 100 to 550°C (with the step of 50°C) in the Aparin's furnace. For the control over possible additional laboratory magnetization of samples, two cubes from the single sample with opposite orientation of two constituting vectors $\mathbf{J_n}$ were placed into the furnace. The Remasoft 3.0 program was used for component processing the data obtained (Chadima and Hrouda, 2006).

Under heating above 200–300°C and impact of fields exceeding 50 mT, low-magnetic samples from the Dvuyakornaya Bay section usually demonstrated additional laboratory magnetization, which provided grounds for the cessation of further magnetic cleaning. In the samples with stronger magnetization from the capes Svyatogo Il'i and Feodosiiskii sections, additional magnetization was unrecognizable up the temperatures of 500–550°C. Therefore, measurements of the characteristic magnetization component (**ChRM**) are largely based on the thermal cleaning results, which are more effective for the examined rock types, for the upper part of the composite section and mainly on the data on demagnetization by the alternating field for the lower part.

As a whole, the results of demagnetization of samples by the alternating field and heating appeared to be well consistent between each other (Fig. 9), which

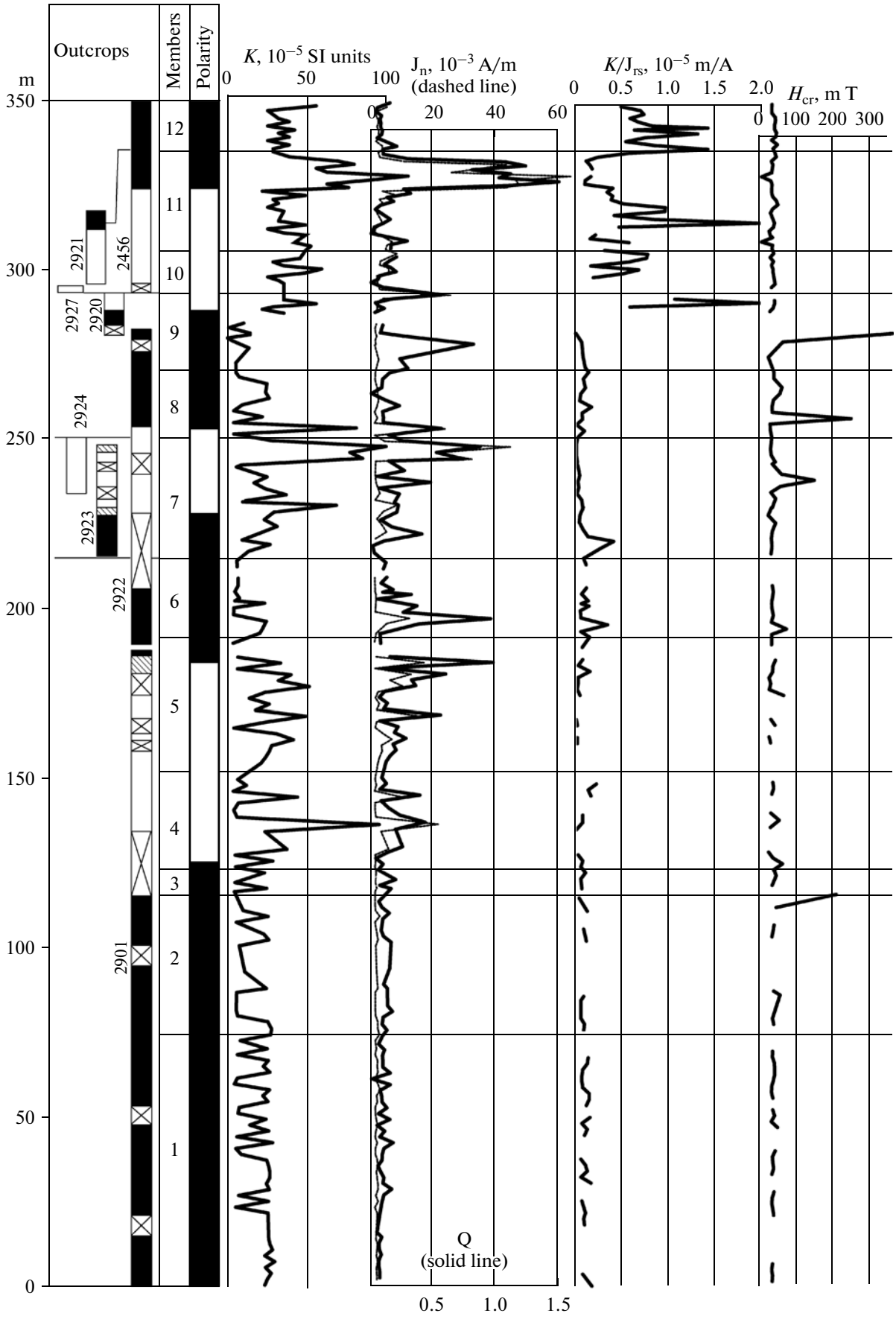

Fig. 8. The composite magnetostratigraphic section of the Tithonian–Berriasian boundary interval in the Feodosiya area: paleomagnetic and petromagnetic characteristics. For legend, see Fig. 3.

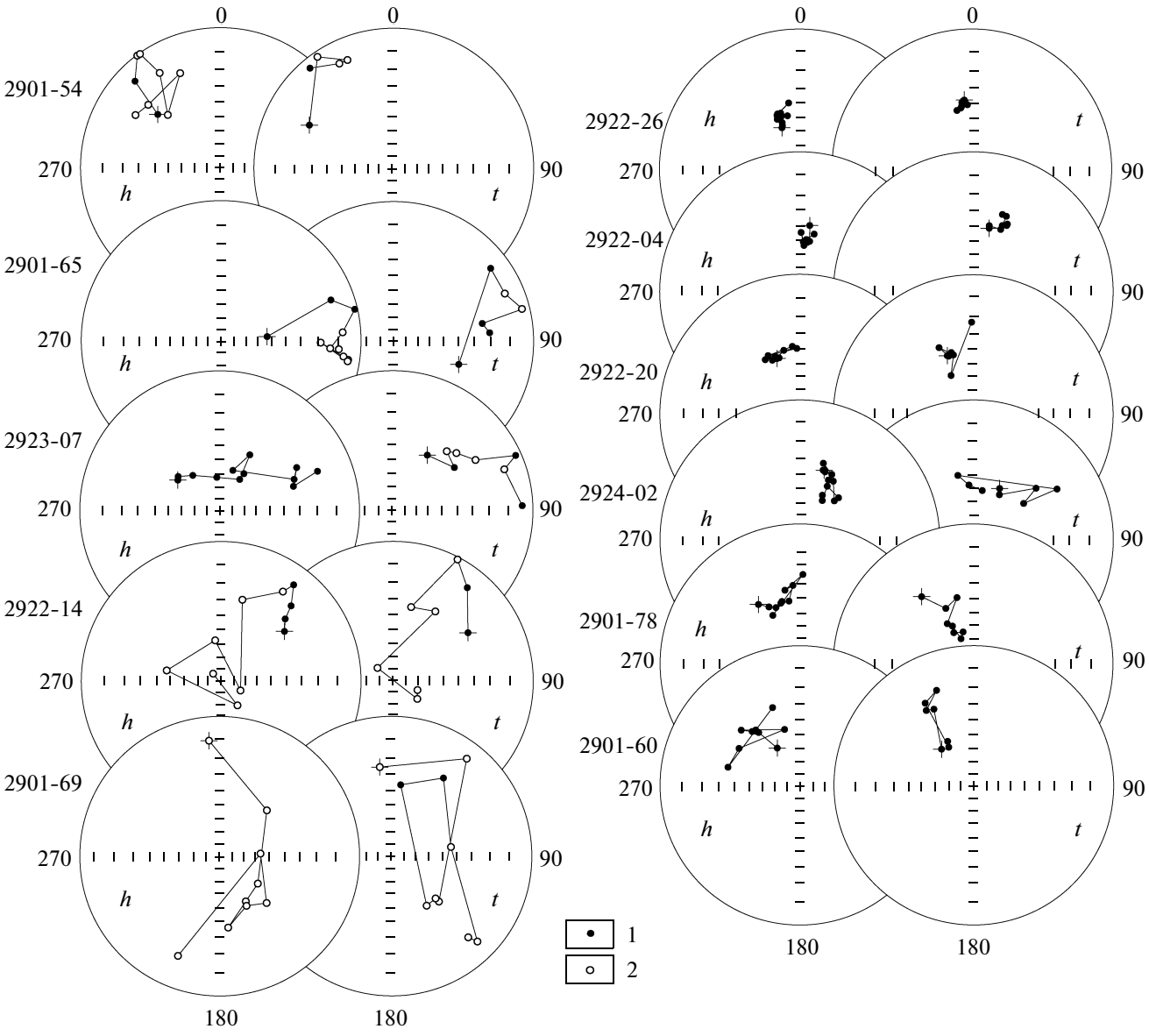

Fig. 9. Comparison of the results of magnetic cleaning by the alternative field (*h*) and heating (*t*). Stereographic projections of changes in $\mathbf{J_n}$ directions during magnetic cleaning are given in the stratigraphic coordinate system.
(1) $\mathbf{J_n}$ projection on the lower hemisphere; (2) $\mathbf{J_n}$ projection on the upper hemisphere.

substantially increases the reliability of paleomagnetic measurements relative to the results based only on one of magnetic cleaning procedures. In most cases, the samples demonstrated two components: low-temperature (**LTC**) or low-coercivity (**LCC**) component in the range of 100 to 200°C or 3 to 15 mT, respectively and high-temperature (**HTC**) or high-coercivity (**HCC**) one after heating above 250°C or after impact of fields exceeding 20 mT (Fig. 10). **LTC** and **LCC** are usually close to the direction of rock remagnetization by the present-day field (remagnetization "cross"), which implies their soft nature. **HTC** and **HCC** are characteristic magnetization components, which were used for determining the magnetic polarity after screening vectors that differed from the direction of the present-day field by <15°. Their precision parameter in the geographic coordinate system is four times higher as compared with that in the stratigraphic coordinate system, which unambiguously indicates the post-folding (viscous) nature of magnetization (Fig. 11). Moreover, it is conceivable that coincidence of some characteristic components $\mathbf{J_n}$ with the "cross" is incidental, and they were wrongly excluded from further consideration.

It was believed that **ChRM** projections that are grouped in northern and northwestern segments of the lower hemisphere correspond to the normal polarity of the geomagnetic field (N), while their counterparts,

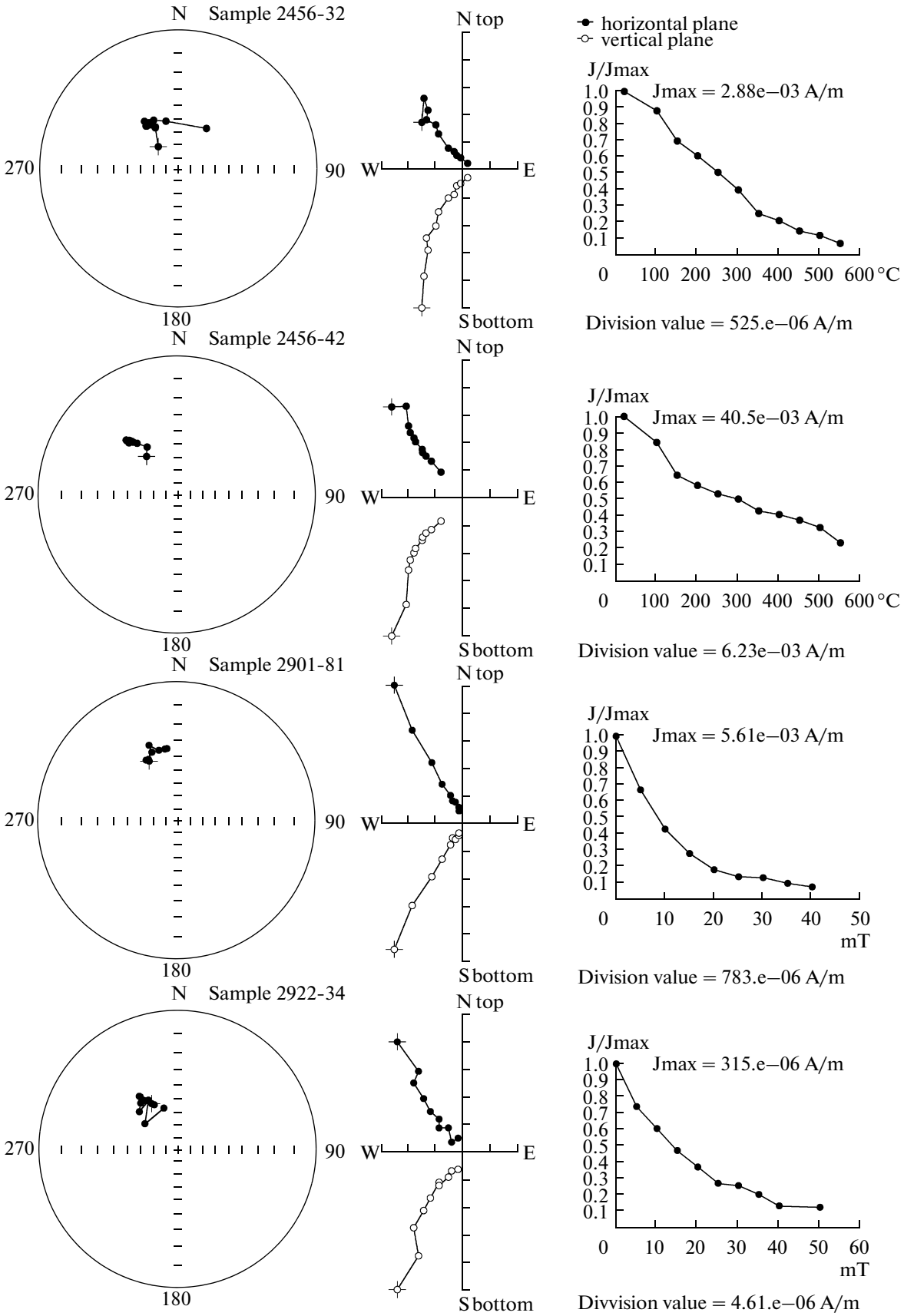

Fig. 10. The results of the component analysis (from left rightward): stereographic illustrations of changes of $\mathbf{J_n}$ vectors during cleaning by the alternating field, Zijderveld diagrams (in the geographic coordinate system, and plots of sample demagnetization. For legend, see Fig. 9.

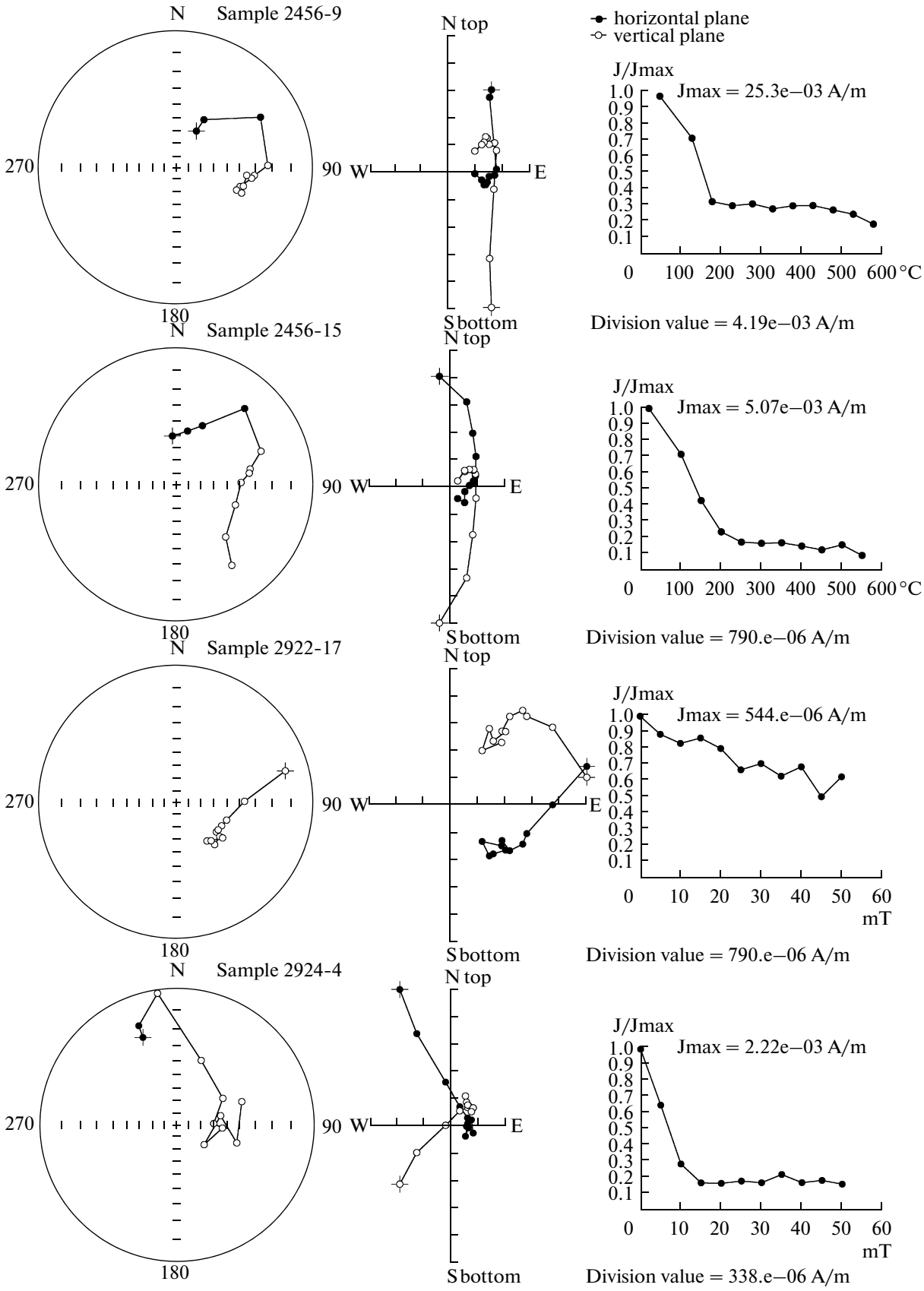
N
Sample 2456-9
270
90
180
W
E
N top
S bottom
horizontal plane
vertical plane
J/Jmax
Jmax = 25.3e–03 A/m
1.0
0.9
0.8
0.7
0.6
0.5
0.4
0.3
0.2
0.1
0
100
200
300
400
500
600 °C
Division value = 4.19e–03 A/m
N
Sample 2456-15
270
90
180
W
E
N top
S bottom
J/Jmax
Jmax = 5.07e–03 A/m
1.0
0.9
0.8
0.7
0.6
0.5
0.4
0.3
0.2
0.1
0
100
200
300
400
500
600 °C
Division value = 790.e–06 A/m
N
Sample 2922-17
270
90
180
W
E
N top
S bottom
J/Jmax
Jmax = 544.e–06 A/m
1.0
0.9
0.8
0.7
0.6
0.5
0.4
0.3
0.2
0.1
0
10
20
30
40
50
60
mT
Division value = 790.e–06 A/m
N
Sample 2924-4
270
90
180
W
E
N top
S bottom
J/Jmax
Jmax = 2.22e–03 A/m
1.0
0.9
0.8
0.7
0.6
0.5
0.4
0.3
0.2
0.1
0
10
20
30
40
50
60
mT
Division value = 338.e–06 A/m

Fig. 10. (Contd.)

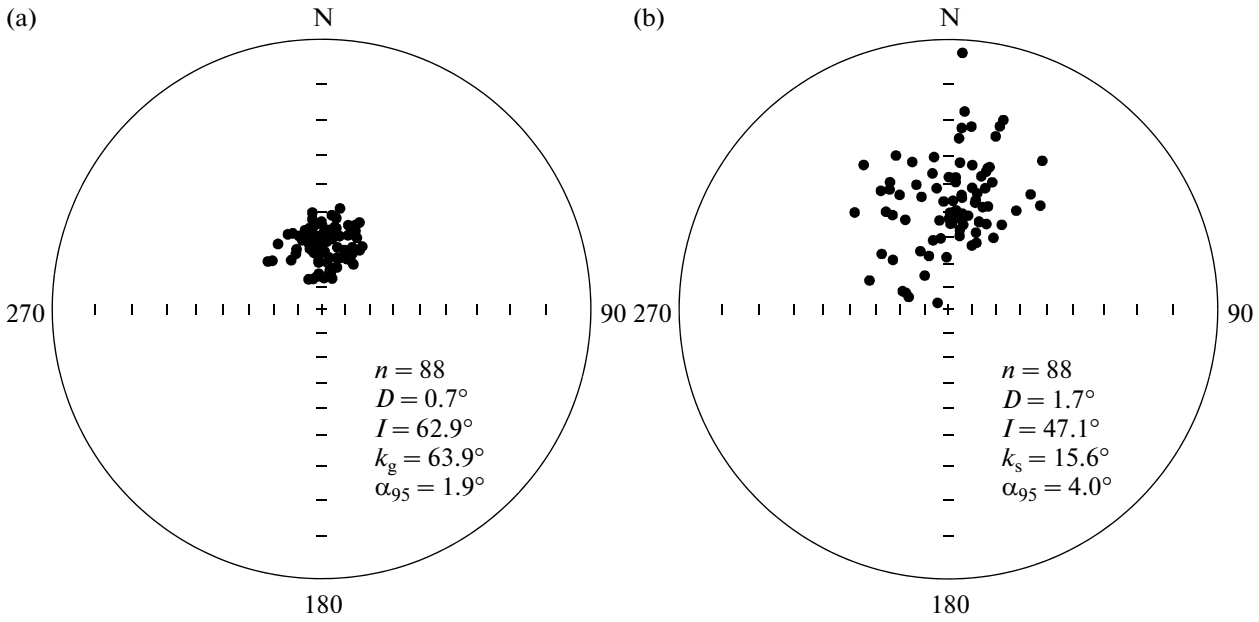

Fig. 11. Stereographic projections of low-coercivity (**LCC**) and low-temperature (**LTC**) components in the geographic (a) and stratigraphic (b) coordinate systems.

For legend, see Fig. 9; for designations of statistic paleomagnetic parameters, see Table 2.

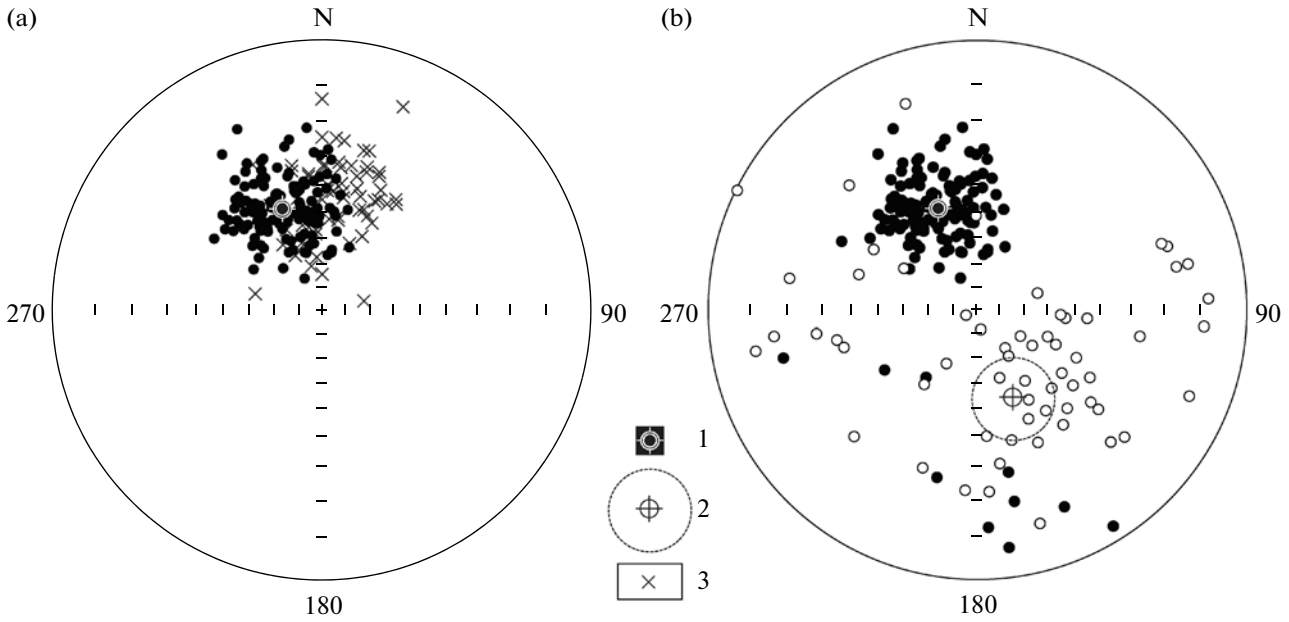

Fig. 12. Stereographic projections of **ChRM** (in the stratigraphic coordinate system): totalities corresponding to the normal polarity (a), normal and reversed polarities (b).

(1, 2) projections of average **ChRM** directions for totalities of N and R vectors, respectively; (3) projection of directions of rock remagnetization by the present-day field (remagnetization "crosses"). For other symbols, see Fig. 9.

which demonstrated a tendency for concentration in southern segments of the upper hemisphere, correspond to the reversed polarity of the geomagnetic field (R) (Fig. 12). Many directions are anomalous: for example, directions with northern declinations and negative inclinations or located in southern quadrants of stereograms and characterized by steep positive inclinations. In such situations, when determining the polarity sign, we took into consideration a trend in changes of the vector $\mathbf{J_n}$ during magnetic cleaning pro-

cedures and used the angle Δ between **ChRM** and syn-fold magnetization component of Tithonian–Berriasian age (**SYN**) as an additional criterion: D = 344°, I = 51° previously defined in the Dvuyakornaya Bay section (Pecherskii and Safonov, 1993). The last authors determined the **SYN** vector by introducing the "intermediate" correction for the bed incline, under which the precision parameter of characteristic magnetization components was maximal. This provided grounds for "speaking about significant contribution of the syn-folding component to remanent magnetization and correlating the defined paleomagnetic direction with the period of sediment deformation" (Pecherskii and Safonov, 1993). Taking into consideration the results of the analysis of the magnetic anisotropy (Bagaeva et al., 2010; this work), we believe that the syn-folding component associates with clays that were subjected to plastic deformations at the diagenesis stage and is, in fact, postsedimentary in origin. Judging from the magnetic anisotropy, most intensely deformed clays constitute the basal part of the Dvuyakornaya Bay section (Fig. 8g).

When the angle Δ counted out in the eastern (E) or western (W) directions from **SYN** exceeded 90° and projection $\mathbf{J_n}$ was regularly displaced during heating procedures southward and/or to the upper hemisphere, **ChRM** was considered to be determined by the vector sum of the incompletely destroyed "hard" component and initial R component. When this angle was <90°, the polarity was accepted to be anomalous. The half of the paleomagnetic column width acquired the polarity sign in the case, when samples with the opposite polarity were located both above and below this interval.

The magnetic polarity columns compiled for each outcrop (Figs. 3–6) were integrated into a composite paleomagnetic column consisting of seven alternating magnetozones: four with the normal polarity and three with the reversed one (Fig. 8). When compiling the composite column, we ignored gaps in the polarity measurement, intervals with the anomalous polarity, and single intervals with the opposite sign against the background of the dominant polarity.

The different degree of **ChRM** "contamination" by the stabilized secondary component related to oxidation products of magnetite grains results in the very wide scatter of R vectors and less affects paleomagnetic statistics of normally magnetized samples (Fig. 12, Table 2) since directions of the present-day and past geomagnetic fields of the normal polarity are similar to each other. During deriving components from the Zijderveld diagrams (Fig. 10), **HTC** and **HCC** corresponding the normal polarity are characterized by maximal angle deviation $MAD < 10°$ (mostly from 2° to 8°), while R components demonstrate $MAD > 15°$ (up to 25°). The poor quality of **ChRM** corresponding to the reversed polarity is partly explained by low $\mathbf{J_n}$ values under high fields and temperatures (approximately 10^{-5}–10^{-6} A/m, i.e., at the sensitivity threshold of the measuring equipment). Nevertheless, the reversal test (Mc Fadden and McElhinny, 1990) performed both for the entire section and its two large intervals (members 1–9 and 9–12) is positive (Table 2), i.e. directions averaged for all **ChRM** corresponding to normal and reversed polarities are statistically identical to their antipodes at the 90% significance level. This indicates the incidental, not systemic character of "contamination" by the characteristic component in representative sample selections taken from beds with different attitude elements.

The **ChRM** directions averaged for all the N and R vectors substantially differ from the average direction of rock remagnetization by the recent field (**RF**) for nine outcrops (Table 2). In each of these outcrops, attitude elements of beds are similar to each other, while they substantially differ in different outcrops. The amplitude of the secular geomagnetic variations of 10° (according to Bakhmutov (2006), the 1200-year variation is characterized by the magnitude equal to 8°) was accepted to represent a radius of the confidence circle at the 95% significance level (α_{95}).

At the same time, the **ChRM** vectors averaged for the whole totalities of N polarities significantly differ from the syn-folding component (Pecherskii and Safonov, 1993), which was accepted as the standard one (Table 2). The average R directions of **ChRM** characterized by extremely large confidence intervals ($\alpha_{95} = 12.1°$–$16.6°$) appear to be statistically identical to **SYN** (Table 2).

In many cases, $\mathbf{J_n}$ directions were regularly displaced during magnetic cleaning procedures along arches of great circles (GC) (Fig. 10), which provides, along with significant variations in attitude elements of beds in the composite section, prerequisites favorable for applying the GC intersection method (Halls, 1976) to determine the more exact **ChRM** direction. For approximation of trajectories of direction changes during magnetic cleaning procedures, we used at least four points (usually 5–8 points). The displacement of magnetization vector projections along great circles is mostly observable in samples, which contain the characteristic component corresponding to the reversed polarity (Fig. 10).

In the stratigraphic coordinate system, all the calculated circles intersect at the point significantly differing from present-day field and statistically corresponding to the **SYN** projection, according to (Debiche and Watson, 1995) (Table 2, Fig. 13). We consider the direction derived from the GC intersection as representing the most reliable **ChRM** vector. This direction is stable: GC screening according to different criteria produces no substantial shifts of the latter affecting only *MAD* (Table 2, Fig. 13).

Summing up the results of paleo- and petromagnetic investigations of the section, let us analyze them

Table 2. Statistical parameters of the **ChRM** vectors distribution

(n) number of samples in the selection, (D_{av}, I_{av}) average paleomagnetic declination and inclination, respectively, (α_{95}) radius of the vector confidence circle, (*MAD*) maximal angle deviation			Polarity	n	D_{av} (°)	I_{av} (°)	α_{95} or *MAD* (°)	Angle with **RF** (°)	Angle with **SYN** (°)	k_s	k_s/k_g	Reversal test results (McFadden and McElhinny, 1990)		
												A (°)	A_c (°)	Cl.
ChRM, derived	from Zijderveld diagrams	Whole section	N-	135	338.4	46.5	2.5	21.1 ± 7.4	5.4 ± 4.3	25.52	1.18	1.8	11.9	C
			R-	101	159.3	–48.2	12.1	20.1 ± 10.2	4.1 ± 8.2	2.35	1.01			
		Dvuyakornaya Bay (outcrops 2901, 2922–2924)	N-	75	342.4	43.7	3.2	18.8 ± 7.6	7.0 ± 4.6	26.60	1.31	6.0	16.9	C
			R-	26	163.1	–49.6	16.6	17.0 ± 13.2	1.5 ± 11.8	3.91	1.02			
		Cape Svyatogo Il'i–Cape Feodosiiskii (outcrops 2456, 2921, 2927)	N-	60	332.9	49.7	3.5	24.5 ± 7.6	6.8 ± 4.7	28.33	1.17	5.1	12.7	C
			R-	52	152.3	–44.7	12.2	25.4 ± 10.9	8.9 ± 9.1	3.61	1.02			
	from GC intersection	GC with *MAD* < 20°		73	345.9	50.7	22.1	15.3 ± 12.7	1.2 ± 11.2					
		GC with *MAD* < 15°		67	342.5	50.4	23.4	17.5 ± 13.2	1.1 ± 11.7					
		GC with *MAD* < 15°, except for landslides		53	345.4	48.1	19.6	15.3 ± 13.1	3.0 ± 11.6					
		GC with *MAD* < 10°		49	343.7	49.5	15.1	16.8 ± 11.9	1.5 ± 10.3					
		GC with *MAD* < 10°, except for landslides		44	344.0	51.9	12.3	17.1 ± 11.0	0.9 ± 9.2					
		GC with *MAD* < 10°, except for landslides		41	340.4	49.3	13.9	19.1 ± 11.7	2.9 ± 10.0					
"Syn-folding" component (**SYN**) (Pecherskii and Safonov, 1993)				50	344	51	5	17.4 ± 8.1						
Average direction of rock remagnetization by the recent field (**RF**)				9	9.2	44.9	10		17.4 ± 8.1					

(k_s/k_g) ratio between interbed paleomagnetic precision parameters in the stratigraphic and geographic coordinate systems, respectively,

(A) angle between average N and R vectors,

(A_c) critical angle,
(Cl.) classification after (McFadden and McElhinny, 1990).

Note: (1) α_{95} are given for **ChRM** derived from the Zijderveld diagrams; **RF**, **SYN**; ***MAD***) for **ChRM** determined by the GC intersection; (2) for **RF**, number of outcrops is taken as n, the maximal amplitude of secular variations (Bakhmutov, 2006) is accepted as α_{95}; (3) prior to calculating angles between vectors, R directions were normalized to the normal polarity (rotated by 180°); (4) angles formed by **ChRM** vectors and **RF** or **SYN** are given with errors (±) determined by statistics of these vectors, according to (Debiche and Watson, 1995). When the angle exceeds an error, vectors differ significantly; when they are lower, vectors statistically coincide with each other (Debiche and Watson, 1995).

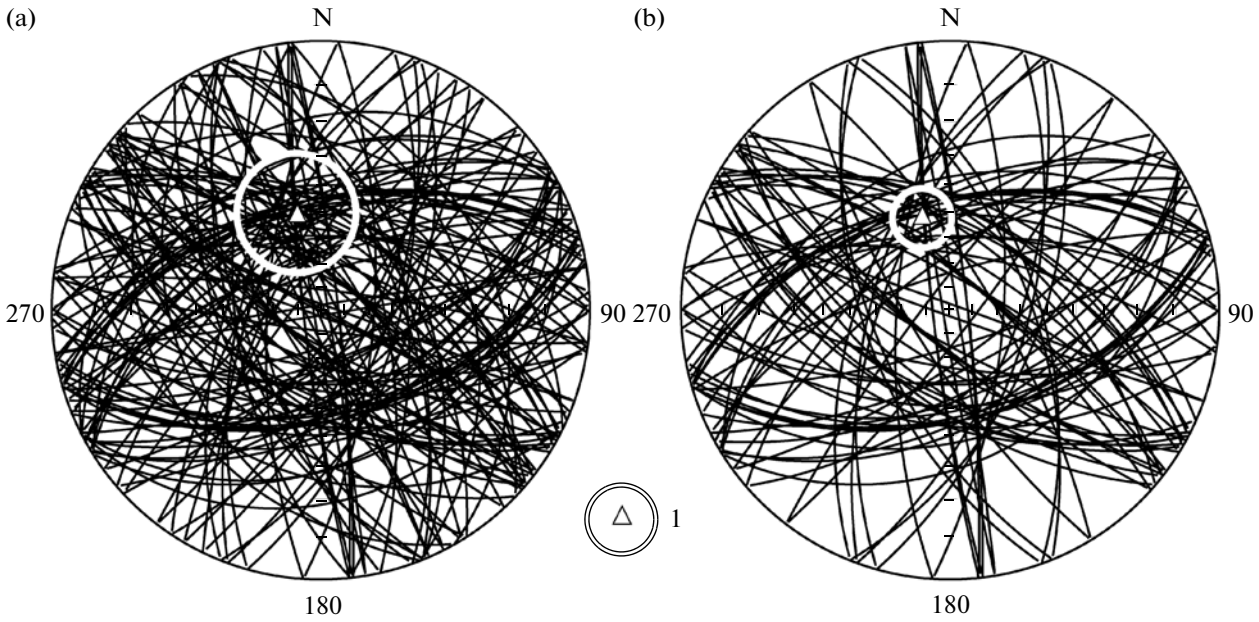

Fig. 13. ChRM values directions determined by the method of great circle (GC) intersection in the stratigraphic coordinate system: (a) using all the GC with $MAD < 20°$; (b) after exclusion GK with $MAD > 10°$ and samples taken from section intervals with landslide displacement features (Table 2).

(1) intersection point of GC with the confidence interval (radius of the circle is equal to *MAD*).

in the context of their consistency with the assumed old age (primary nature) of magnetization.

(1) The paleomagnetic column of the section is represented by large regularly alternating magnetozones with signs of the geomagnetic field being indifferent to both lithology and variations in petromagnetic characteristics (Figs. 3–6, 8), which is consistent with the hypothesis of the geophysical nature of these zones. The inversion of the magnetic field is a phenomenon of the global scale; therefore, in the particular section the probability of interrelation between magnetic polarity and lithological–magnetic characteristics determined by local and regional factors is extremely low in case of primary nature of magnetization and lack of breaks in sedimentation.

(2) The substantiation of the $\mathbf{J_n}$ orientation (post-orientation) nature is identical to substantiation of its primary nature. The section under consideration demonstrates features, which are characteristic of detrital magnetization and, to the contrary, untypical of chemical magnetization:

—low Q factor values largely equal to fractions of a unit (Fig. 8). Values of $Q \geq 1$ are registered only a six levels; so even with their screening, the paleomagnetic structure of the composite column should remain generally the same;

—paleomagnetic interbed precision parameters are relatively low never exceeding several tens of units (Table 2);

—judging from the DTMA and magnetic saturation data, partly oxidized allothigenic magnetite is the most probable magnetization carrier.

(3) In the situation under consideration, the lack of positive results of the fold test cannot serve a cause for rejecting the magnetic-polarity interpretation of the data obtained by the component analysis. Taking into consideration the data in (Pecherskii and Safonov, 1993) on the contribution of syn- and post-folding components to magnetization, our data demonstrating the statistically insignificant difference between paleomagnetic precision parameters along the section in stratigraphic (k_s) and geographic (k_g) coordinate systems seem natural (Table 2). The incorrectness of the fold test is explained by both incomplete destruction of the secondary component and disregard of the incline of the initial surface and synsedimentary clay deformations. The fact that clayey sediments under consideration were deposited on the steep ramp slope, not on the horizontal surface and they were involved in viscous–fluid displacements is consistent with both sedimentological and petromagnetic data. The analysis of the data on the magnetic anisotropy (Bagaeva et al., 2010) reveals that clays are deformed more intensely compared with limestones. Nevertheless, the top of the nearest compact limestone bed was forcedly accepted to represent the clay bedding surface, which could result in erroneous determination of attitude elements of clayey beds.

(4) The positive inversion (reversal) test (Table 2) serves as evidence in favor of the primary magnetization nature.

(5) The significant differences of averaged **ChRM** vectors determined by different methods from the direction of the present-day field are also consistent, with account for its possible secular variations (Table 2), with the hypothesis of the primary magnetization nature. We consider the use of defined characteristic components for calculating the virtual geomagnetic pole incorrect, since the real angle of the ramp slope, where the sediments were deposited, remains unknown.

(6) The "criterion of the external convergence," i.e. identity of the paleomagnetic structure of coeval sediments in remote sections is the most important feature that favors the hypothesis of the primary magnetization nature. The greater the difference between lithological–facies characteristics of the correlated sections, the more significant is the criterion of the external convergence indicating the primary $\mathbf{J_n}$ nature.

The paleomagnetic zonality of the composite Crimean section is very consistent with accepted views on the polarity-variable geomagnetic field at the Tithonian–Berriasian transition, which are based on both linear magnetic anomalies and evidence from reference sections (Channell et al., 1995; Ogg and Ogg, 2008) (Fig. 14). The magnetic polarity characteristics of the Jurassic–Cretaceous boundary interval substantiated by microfaunal data are obtained in the Carpathians of Slovakia (Houša et al., 1997), Poland (Grabowski and Pszczółkowski, 2006), Hungary (Grabowski et al., 2010), the Alps of Italy (Houša et al., 2004, Channell et al., 2010) and Austria (Likeneder et al., 2010) (Fig. 14). The Puerto Escano section (southern Spain), where magnetozones are correlated with both microfaunal (calpionellid) and ammonite zones (Pruner et al., 2010) occupies a particular place among Tithonian–Berriasian magnetostartigraphic sections of West Europe (Fig. 14). Thus, the Jurassic–Cretaceous boundary transition is one of the Mesozoic intervals best studied with respect to its paleomagnetic characteristics at least in the Tethyan realm. Such integrated bio- and magnetostratigraphic data on boreal age analogs are now available only for the Nordvik Peninsula in northern Siberia (Houša et al., 2007). In all the sections, the upper Tithonian–basal Berriasian interval (Macrocanthum, Durangites, and Jacobi ammonite zones; Chitinoidella, Crassicollaria, and Calpionella calpionellid zones; NJT16, NJT17, and NKT nannofossil zones) or uppermost Volgian–basal Boreal Berriasian stages correspond to several different-polarity magnetozones, which are identified with the succession of M20n to M17r magnetochrons (Fig. 14).

All the above-mentioned items are best explained by the magnetization formation both during sedimentation and at the diagenesis stage, which was accompanied by plastic deformations of clayey sediments. This conclusion is also consistent with the results of tests, which indicate the primary nature of the characteristic component, and data on syn-folding **ChRM** age, while all of them together provide reliable evidence in favor of the postorientation $\mathbf{J_n}$ nature.

There are several systems of criteria developed by different authors for assessing the reliability of paleomagnetic data (Van der Voo, 1993; Opdyke and Channell, 1996; *Dopolneniya...,* 2000; and others. Differing in some details, all of them include requirements in common such as reliably substantiated age of the examined samples, their sufficient number, qualitative magnetic cleaning procedures, component analysis, succession of different-polarity magnetozones, and others.

The index of the paleomagnetic confidence for the section under consideration is as high as six points (of seven possible), according to the classification in (Van der Voo, 1993), eight (of 10 possible) and seven (of eight possible), according to confidence criteria adapted for magnetostratigraphic purposes in (Opdyke and Channell, 1996) and seven (of eight possible) by A.N. Khramov in (*Dopolneniya...*, 2000), respectively. The maximal index values were never reached because of the section location beyond the craton (Van der Voo, 193), lack of radiometric dates (Opdyke and Channel, 1996; *Dopolneniya...*, 2000), and disregard of the least square method during determining paleomagnetic directions (Opdyke and Channel, 1996; *Dopolneniya...,* 2000).

Thus, despite the generally low paleomagnetic quality of examined rocks, which provides grounds for doubting polarity determination for particular samples, the magnetostratigraphic result in the form of the paleomagnetic column deserves confidence.

STRATIGRAPHIC CORRELATION

The Crimean Tithonian–Berriasian section is primarily correlated using magnetostartigraphic data with the Puerto Escano section (Pruner et al., 2010), not with the magnetochronological scale (Ogg and Ogg, 2008) since boundaries of ammonite zones in the latter are correlated with magnetozones indirectly through correlation with microfaunal zones. Such a procedure is ambiguous for several reasons, one of which consists of significant diachronism of microfaunally substantiated boundaries. For example, in Southern Alps sections, which are located at distances never exceeding 150 km from each other (Channell et al., 2010), the boundary between NJT17 and NKT nannofossil zones occupies different positions relative to magnetochrons ranging from the top of M19n to top of M18n (Fig. 14).

Correlation with the Puerto Escano magnetostratigraphic section shows that the paleontologically barren Member 1 with the normal polarity represent an age analog of the upper Tithonian Microcanthum Zone, since the uppermost lower Tithonian section is largely characterized by the reversed polarity (Chron M20r). Member 2 belonging to the same zone was previously substantiated by finds of the ammonite species *Oloriz-*

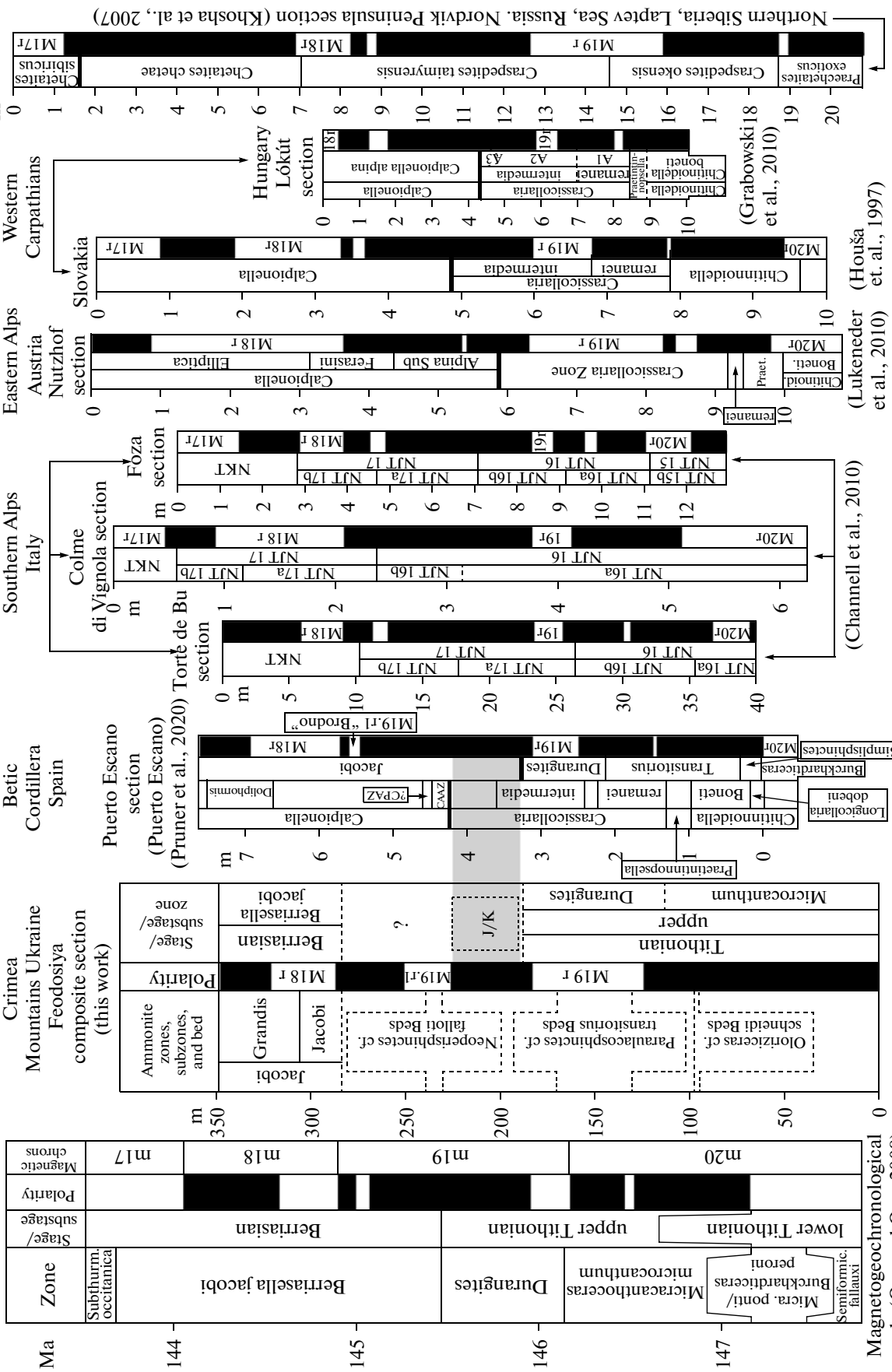

Fig. 14. Correlation of magnetostratigraphic data on the Jurassic–Cretaceous boundary interval from different regions. The solid line shows the Tithonian–Berriasian boundary in the magnetochronological scale and Tethyan sections and Volgian–Boreal Berriasian boundary in the boreal Nordvik section. In the composite Feodosiya section, dashed rectangle with the J.K index designates an interval, where the Jurassic–Cretaceous boundary should be placed, according to the magnetostratigraphic correlation with the Puerto Escano section.

iceras cf. *schneidi* (Arkad'ev, 2004; Arkad'ev et al., 2008).

Based on finds of *Paraulacosphinctes* cf. *senoides* Tavera and *P.* cf. *transitorius* (Oppel), members 4 and 5 were initially attributed to the Transitorius Subzone of the Microcanthum Zone, although representatives of the genus *Paraulacosphinctes* are also known from the Durangites Zone (Enay and Geyssat, 1975). Judging from magnetostratigraphic data, Member 4 corresponds to the Durangites Zone (Arkad'ev et al., 2010) since it is located within the reversed-polarity magnetozone, which may represent only an analog of Chron M19r. No other large magnetozones are known in the upper Tithonian interval.

In the magnetochronologic scale, reversed-polarity Chron M19 is followed by Subchron M19n.1r ("Brodno") (Fig. 14). Therefore, the overlying magnetozone of the opposite polarity corresponding to Member 7 is identified precisely with the latter despite the find of the ammonite species *Neoperisphinctes* cf. *falloti*, which was previously known only from the upper Tithonian of Spain, at the base of the R zone, while the "Brodno" episode in the Puerto Escano section is located within the Berriasian Jacobi Zone (Fig. 14). The alternative identification of the R magnetozone, which characterizes Member 7, is impossible, without assuming unknown long reversed-polarity epochs in the late Tithonian. In the Crimean section the assumed analog of Subchron M19n.1r is characterized by the untypically anomalous thickness comparable with that of R subzones (analogs of Chrons M16r and M19r), which is probably explained by the increased sedimentation rates during the geomagnetic "Brodno" episode. Such thickness proportions of the subzone and microzone (analogs of Chron M19r and Subchron "Brodno," respectively) are registered, for example in the Lókút section of Hungary (Grabowski et al., 2010) (Fig. 14).

The first representatives of Berriasian ammonites (*Ptychophylloceras* sp., and *Delphinella* cf. *tresannensis* Le Hégarat) that characterize the Jacobi Zone are found in the uppermost layers of Member 9 (Cape Feodosiiskii, 2010). Higher in the section, sediments contain ammonite assemblages, which indicate the presence of the Jacobi and Grandis zones. The long reversed-polarity magnetozone traceable from the top of Member 9 to the top of Member 11 is a doubtless analog of Chron M18r, since no other R magnetozones are known in this Berriasian interval.

In the Puerto Escano section, the Jacobi Zone is not divided into subzones. At the same time, by analogy with the Feodosiya section, where the Jacobi–Grandis boundary is confined to Chron M18r, it may be concluded that the Doliformis calpionellid subzone of southern Spain corresponds to the Grandis Subzone (Fig. 14).

By analogy with Tethyan sections, where the Jurassic–Cretaceous boundary is substantiated by both ammonites (at the base of the Jacobi Zone) and calpionellids (at the base of the Calpionella Zone), the boundary between these systems in the Feodosiya section should be placed in the lower part of Chron M19n, i.e., between the top of M19r and base of Chron M19n.1r (Fig. 14). In this connection, the Neoperisphinctes cf. falloti Beds should be attributed to the Berriasian, although this conclusion is premature, since the solution of the problem of the Jurassic–Cretaceous boundary location both in Crimea and other regions is limited by the selection of criteria for its defining. The reasonability of the complex biostratigraphic substantiation of the Tithonian–Berriasian boundary casts no doubt. At the same time, such an approach reveals the inconsistency of the boundaries defined by different faunal and floral groups, which is aggravated by diachronism of various reference levels used for correlation. Such a situation is illustrated by the Puerto Escano section, where the Jurassic–Cretaceous boundary defined by ammonites and calpionellids is placed at different levels (Pruner et al., 2010) and sections in the Southern Alps, which demonstrate different relationships between nannofossil zones and magnetic chrons (Channell et al., 2010) (Fig. 14). As compared with biotic events, levels of magnetic inversions are undoubtedly more isochronous; therefore, they should be used, along with paleontological features, for substantiating boundaries between units of the general stratigraphic scale in particular sections giving preference to the inversion, which is readily recognizable and closest to the biostratigraphic boundary in the stratotype (Guzhikov and Baraboshkin, 2006). The base of Subchron M19n.1r may be recommended as a criterion for determining the Jurassic–Cretaceous boundary. When the "Brodno" episode is unrecognizable, either the top of Chron M19r as a level nearest to the boundary between the Durangites and Jacobi zones in the Puerto Escano reference section (Pruner et al., 2010) or base of Chron M18r, as was proposed in (Channell et al., 2010), should be used. Nevertheless, the selection of the paleomagnetic criterion should be preceded by the ultimate solution of the problem related to the paleontological substantiation of the Jurassic–Cretaceous boundary.

CONCLUSIONS

(1) The investigation of upper Tithonian–Berriasian sediments in the Feodosiya area resulted in the compilation of their continuous composite section with the detailed bed-by-bed description, sedimentological interpretation, and substantiation of its complete stratigraphic record.

(2) The succession of upper Tithonian ammonite assemblages is first established; ammonites found in this section made it possible to specify the positions of the Berriasian Jacobi Zone and Grandis Subzone bases.

(3) It is shown that the upper Tithonian–Jacobi Zone interval in Crimea contains continuous record of

magnetozones, which are identified with magnetic chrons M20n, M19, M18 and Subchron M19n.1r. The bio- and magnetostratigraphic correlation of the Feodosiya section with Tithonian–Berriasian boundary intervals of southern Spain and other regions revealed in the former age analogs of standard ammonite zones of West Europe: Microcanthum, Durangites, and Jacobi.

ACKNOWLEDGMENTS

We are grateful to reviewers M.A. Rogov (Geological Institute, Russian Academy of Sciences) for his help in identifying upper Tithonian ammonites and A.Yu. Kazanskii (Institute of Petroleum Geology and Geophysics, Siberian Branch, Russian Academy of Science) for editing the manuscript and for valuable recommendations concerning the magnetostratigraphic section of the article. This work was supported by the Russian Foundation for Basic Research (project nos. 11-05-00405, 10-05-00276, and 10-05-00308) and Federal Purposeful Program "Scientific–pedagogical personnel of innovated Russia. Activity 1.1. Organization of scientific investigations by teams of scientific–educational centers" (State contract no. 14.740.11.0190).

Reviewers A.Yu. Kazanskii and M.A. Rogov

REFERENCES

Arkad'ev, V.V. and Savel'eva, Yu.N., The Jacobi-Grandis Zone of the Berriasian Stage (Mountain Crimea), in *Problemy biokhronologii v paleontologii i geologii. Tez. Dokl. XLVIII Sess. Paleontol. Ob-va* (Problems of Biochronology in Paleontology and Geology. Proc. XLVIII Session of Paleontol. Soc.), St. Petersburg, 2002, pp. 11–13.

Arkad'ev, V.V., Berriasella Jacobi-Pseudosubplanites Grandis Zone of the Berriasian Stage (Mountain Crimea), *Bull. Mosk. Ob-va Ispyt. Prir., Otd. Geol.*, 2003, vol. 78, no. 6, pp. 29–35.

Arkad'ev, A.A., Fedorova, A.A., Savel'eva, Yu.N., and Tesakova, E.M., Biostratigraphy of Jurassic-Cretaceous Boundary Sediments in the Eastern Crimea, in *2-e Vseross. soveshchanie "Melovaya sistema Rossii: problemy stratigrafii i paleogeografii". Tez. Dokl.* (Cretaceous System of Russia: Problems of Stratigraphy and Paleogeography. Proc. II All-Russian Conf.), St. Petersburg: Izd. SPbGU, 2004, p. 17.

Arkad'ev, V.V., The First Finding of Late Tithonian Ammonite in the Feodosiya Section of the Eastern Crimea, *Paleontol. Zh.*, 2004, no. 3, pp. 39–45.

Arkad'ev, V.V. and Bogdanova, T.N., The Genus Delphinella (Ammonoidea) from Deposits of the Berriasian Stage (Mountain Crimea), *Paleontol. Zh.*, 2005, no. 5, pp. 30–38.

Arkad'ev, V.V., Fedorova, A.A., Savel'eva, Yu.N., and Tesakova, E.M., Biostratigraphy of Jurassic-Cretaceous Boundary Sediments in the Eastern Crimea, *Stratigr. Geol. Correlation,* 2006, vol. 14, no. 3, pp. 302–330.

Arkad'ev, V.V. and Rogov, M.A., New data on Upper Kimmeridgian-Tithonian Biostratigraphy and Ammonites of the Eastern Crimea, *Stratigr. Geol. Correlation*, 2006, vol. 14, no. 2, pp. 185–199.

Arkad'ev, V.V., Bogdanova, T.N., Lobacheva, S.V., et al., The Berriasian Stage of the Crimean Mountains: Zonal Subdivisions and Correlation, *Stratigr. Geol. Correlation*, 2008, vol. 16, no. 4, pp. 400–422.

Arkad'ev, V.V., The Jurassic-Cretaceous Boundary in the Mountain Crimea in *Ocherki po regional'noi geologii. Sb. Nauchn. Trudov* (Outline of Regional Geology. Edited Volume), Saratov: Izd. Tsentr "Nauka", 2008.

Arkad'ev, V.V., Bagaeva, M.I., Guzhikov, A.Yu., et al., New data on the Ammonites and Biostratigraphy of the Kimmeridgain and Tithonian of the Mountain Crimea in *Materialy 5-go Vseross. Sovesh. "Melovaya sistema Rossii i blizhnego zarubezh'ya: problemy stratigrafii i paleogeografii"* (Cretaceous System of Russia and Russia's Neighboring States. Proc. 5th All-Russian Conf.) Baraboshkin, E.Yu. and Blagoveshchenskii, I.V., Eds., Ul'yanovsk: UlGU, 2010, pp. 49–53.

Arkad'ev, V.V., New data on ammonoids of the Genus Paraulacosphinctes from the Upper Tithonian of the Mountain Crimea, *Stratigr. Geol. Korrelyatsiya*, 2011, vol. 19, no. 2, pp. 120–124.

Bagaeva, M.I., Guzhikov, A.Yu., and Yampol'skaya, O.B., The Results of a Study of Anisotropy of Magnetic Susceptibility of Tithonian-Berriasian Sediments of the Mountain Crimea in *Materialy 5-go Vseross. Sovesh. "Melovaya sistema Rossii i blizhnego zarubezh'ya: problemy stratigrafii i paleogeografii"* (Cretaceous System of Russia and Russia's Neighboring States. Proc. 5th All-Russian Conf.) Baraboshkin, E.Yu. and Blagoveshchenskii, I.V., Eds., Ul'yanovsk: UlGU, 2010, pp. 63–66.

Bakhmutov, V.G., *Paleovekovye geomagnitnye variatsii* (Paleosecular Geomagnetic Variations), Kiev: Naukova dumka, 2006.

Baraboshkin, E.Yu., Paleogeography of the East European Platform and its Southern Framework in Early Cretaceous in *Ser. Analytic. Obzorov "Ocherki po regional'noi geologii Rossii"* (Series of Analytical Reviews) Mezhelovskii, N.V., Ed., Moscow: Izd. Geokart, GEOS, 2005, Iss. 1, pp. 201–232.

Baraboshkin, E.Yu. and Yanin, B.T., Ichnofacies Complexes and Conditions of Formation of Jurassic-Cretaceous Boundary in the Eastern Crimea in *Yurskaya Sistema Rossii: problemy stratigrafii i paleogeografii. 4-e Vseross. Soveshch.: Nauchn. Materialy*, (Jurassic System of Russia: Problems of Stratigraphy and Paleogeography. Proc. 4th All-Russian Conf.) Zakharov, V.A. Ed., St. Petersburg: OOO "Izd. LEMA", 2011, pp. 30–32.

Bogdanova, T.N., Lobacheva, S.V., Prozorovskii, V.A., and Favorskaya, T.A., About Subdivision of the Berriasian Stage in the Mountain Crimea, *Vestn. Leningr. Univ., Ser. Geol.-Geogr.*, 1981, vol. 1, no. 6, pp. 5–14.

Bogdanova, T.N., Lobacheva, S.V., Prozorovskii, V.A., and Favorskaya, T.A., The Berriasian Sediments in the Eastern Crimea and the Jurassic-Cretaceous Boundary, in *Pogranichnye yarusy yurskoi i melovoi sistem* (Boundary Stages of Jurassic and Cretaceous Systems), Moscow: Nauka, 1984, pp. 28–35.

Bogdanova, T.N. and Arkadiev, V.V., Revision of Species of the Ammonite Genus Pseudosubplanites from the Berriasian of the Crimean Mountains, *Cretaceous Res.*, 2005, vol. 26, pp. 488–506.

Chadima, M. and Hrouda, F., Remasoft 3.0 a User-Friendly Paleomagnetic Data Browser and Analyzer, *Travaux Geophysiques*, 2006, vol. XXVII, pp. 20–21.

Channell, J.E.T., Erba, E., Nakanishi, M., and Tamaki, K., Late Jurassic-Early Cretaceous Timescales and Oceanic Magnetic Anomaly Block Models, in *Geochronology, Time Scales and Stratigraphic Correlation*, Berggren W.A., Kent, D.V., Aubry, M., and Hardenbol, J., Eds., *SEPM Spec. Publ.*, 1995, vol. 54, pp. 51–63.

Channell, J.E.T., Casellato, C.E., Muttoni, G., and Erba, E., Magnetostratigraphy, Nannofossil Stratigraphy and Apparent Polar Wander for Adria-Africa in the Jurassic-Cretaceous Boundary Interval, *Palaeogeogr. Palaeoclimatol. Palaeoecol.*, 2010, vol. 293, pp. 51–75.

Debiche, M.G. and Watson, G.S., Confidence Limits and Bias Correction for Estimating Angles between Directions with Applications to Paleomagnetism, *J. Geophys. Res.*, 1995, vol. 100, no. B12, pp. 24405–24430.

Dopolneniya k stratigraficheskomu kodeksu Rossii (Additions to the Stratigraphic Code of Russia), St. Petersburg: VSEGEI, 2000 [In Russian].

Drushchits, V.V. and Kudryavtsev, M.P., *Atlas nizhnemelovoi fauny Severnogo Kavkaza i Kryma* (Atlas of Lower Cretaceous Fauna of North Caucasus and Crimea), Moscow: Gostoptekhizdat, 1960 [In Russian].

Drushchits, V.V., *O granitse mezhdu yurskoi i melovoi sistemami. Tezisy doklada* (About the Jurassic-Cretaceous Boundary. Theses), Moscow: Izd. MGU, 1969 [In Russian].

Drushchits, V.V., The Berriasian of the Crimea and Its Stratigraphical Relations, *Colloque sur la limite Jurassique-Crétacé, Lyon, Neuchâtel, Septembre 1973. Memoires de Bureau de recherches géologiques et Minières de France*, Paris, 1975, vol. 86, pp. 337–341.

Enay, R. and Geyssant, J.R., Faunes tithoniques des chaînes bétiques (Espagne Meridionale). Colloque sur la Limite Jurassique-Crétacé (Lyon: Neuchâtel, September 1973), *Mem. Bur. Rech. Geol et Minières*, 1975, vol. 86, pp. 39–55.

Geyssant, J., Tithonien, Biostratigraphie du Jurassique ouest-européen et méditerranéen, Cariou, E. and Hantzpergue, P., Coord., *Bull. Centre Rech. Elf Explor. Prod.*, 1997, Mem. 17, pp. 97–102.

Gorbachik, T.N., Peculiarities of Foraminifera Distribution in Berriasian-Valangian Sediments of the Crimea, *Vestn. MGU, Ser. Geol.*, 1969, no. 6, pp. 58–67.

Gorbachik, T.N., Drushchits, V.V., and Yanin, B.T., Peculiarities of Berriasian and Valangian Basins of the Crimea and Their Populations, *Vestn. MGU, Ser. Geol.*, 1970, no. 3, pp. 16–25.

Grabowski, J. and Pszczółowski, A., Magneto- and Biostratigraphy of the Tithonian-Berriasian Pelagic Sediments in the Tatra Mountains (Central Western Carpathians, Poland): Sedimentary and Rock Magnetic Changes at the Jurassic/Cretaceous Boundary, *Cretaceous Res.*, 2006, vol. 27, pp. 398–417.

Grabowski, J., Haas, J., Marton, E., and Pszczółowski, A., Magneto- and Biostratigraphy of the Jurassic/Cretaceous Boundary in the Locut Section (Transdanubian Range, Hungary), *Stud. Geophys. Geod.*, 2010, no. 54, pp. 1–26.

Guzhikov, A.Yu. and Baraboshkin, E.Yu., Assessment of Diachronism of Biostratigraphic Boundaries by Magneto-chronological Calibration of Zonal Scales for the Lower Cretaceous of the Tethyan and Boreal Belts, *Dokl. Akad. Nauk*, 2006, vol. 409, no. 3, pp. 365–368.

Halls, H.C., A Least-Squares Method to Find a Remanence Direction from Converging Remagnetization Circles, *Geophys. J. R. Astr. Soc.*, 1976, vol. 45, pp. 297–304.

Le Hégarat, G., Perisphinctidae et Berriasellidae de la limite Jurassique-Crétacé. Genres nouveaux et révision critique de quelques définitions taxonomiques antérieures, *C. R. Acad. Sci. Paris*, 1971, Ser. D, vol. 273, no. 10, pp. 850–853.

Hoedemaeker, P.J. and Rawson, P.F., Report on the 5th International Workshop of the Lower Cretaceous Cephalopod Team (Vienna, September 5, 2000), *Cretaceous Res.*, 2000, no. 21, pp. 857–860.

Houša, V., Krs, M., Krsova, M., et al., High-Resolution Magnetostratigraphy across the Jurassic-Cretaceous Boundary Strata at Brodno Near Zilina, Western Carpathians, Western Slovakia, *Mineralia Slovaca*, 1997, no. 29, pp. 312–314.

Houša, V., Krs, M., Man, O., et al., Combined Magnetostratigraphic, Palaeomagnetic and Calpionellid Investigations across Jurassic/Cretaceous Boundary Strata in the Bosso Valley, Umbria, Central Italy, *Cretaceous Res.*, 2004, vol. 25, pp. 771–785.

Khosha, V., Pruner, P., Zakharov, V.A., et al., Boreal-Tethyan Correlation of the Jurassic-Cretaceous Boundary Interval Based on Magneto- and Biostratigraphy, *Stratigr. Geol. Korrelyatsiya*, 2007, vol. 15, no. 3, pp. 63-76.

Kuvaeva, S.B. and Yanin, B.T., Palinological Characteristics of Lower Cretaceous Sediments of the Mountain Crimea, *Vestn. MGU, Ser. Geol.*, 1973, no. 5, pp. 49–57.

Kuznetsova, K.I. and Gorbachik, T.N., *Stratigrafiya i foraminifery verkhnei yury i nizhnego mela Kryma* (Upper Jurassic and Lower Cretaceous Stratigraphy and Foraminifera Species in the Crimea), Moscow: Nauka, 1985 [In Russian].

Lobacheva, S.V. and Smirnova, T.N., Diversity of Berriasian Brachiopods of Crimea, in *1-e Vseross. Soveshch. "Melovaya sistema Rossii: problemy stratigrafii i paleogeografii" (Moskva, 4–6 fevr. 2002 g.). Tez. dokl.* (Cretaceous System of Russia: Problems of Stratigraphy and Paleogeography. Proc. 1st All-Russian Conf.), Moscow: Izd. Mosk. Gos. Univ., 2002, pp. 48–49.

Lobacheva, S.V. and Smirnova, T.N., Berriasian (Lower Cretaceous) Brachiopods from the Crimea, *Stratigr. Geol. Correlation*, 2006, vol. 14, no. 6, pp. 642–654.

Lukeneder, A., Halasova, E., Kroh, A., et al., High Resolution Stratigraphy of the Jurassic-Cretaceous Boundary Interval in the Gresten Klippenbelt (Austria), *Geologica Carpathica*, 2010, vol. 61, no. 5, pp. 365–381.

Matveev, A.V., Tithonian Calcareous Nanoplankton of the Eastern Crimea, in *Iskopaemaya fauna i flora Ukrainy: paleoekologicheskii i stratigraficheskii aspekty. Biostratigrafiya, paleontologiya. Mezozoi* (Fossil Fauna and Flora of the Ukraine: Paleoecological and Stratigraphic Aspects. Biostratigraphy, Paleontology. Mesozoic), Kiev: Inst. Geol. Nauk NAN Ukrainy, 2009, pp. 104–107.

Matveev, A.V., Lower Berriasian Calcareous Nanoplankton of the Mountain Crimea, in *Materialy 5-go Vseross. Soveshch. "Melovaya sistema Rossii i blizhnego zarubezh'ya: problemy stratigrafii i paleogeografii" (23–28 avgusta 2010 g.,*

Ul'yanovsk) (Cretaceous System of Russia and Russia's neighboring states. Proc. 5th All-Russian Conf.) Baraboshkin, E.Yu. and Blagoveshchenskii, I.V., Eds., Ul'yanovsk: UlGU, 2010, pp. 251–256.

Muratov, M.V., Geological Sketch of Eastern End of the Crimea Mountains, *Tr. MGRI*, 1937, vol. 7, pp. 21–122.

Pecherskii, D.M. and Safonov, V.A., Paleomagnetic Palinspastic Reconstruction of the Mountain Crimea Position in Middle Jurassic–Early Cretaceous, *Geotektonika*, 1993, no. 1, pp. 96–105.

Platonov, E.S. and Arkad'ev, V.V., The Jurassic-Tethyan Boundary in the Eastern Crimea, Distinguished on Ammonites and Tintinnides, in *Rates of Evolution of Organic World and Biostratigraphy*, in *Materialy LVII Sess. Paleontol. Ob-va pri RAN* (Proc. LVII Session of Paleontol. Soc. of RAS), St. Petersburg, 2011, pp. 98–100.

Sazonova, I.G. and Sazonov, N.T., Comparative Stratigraphy and Fauna of Jurassic-Cretaceous Boundary Lauers in Eastern Europe. Geology and Oil and Gas Occurrence Peri-Caspian Depression, *Tr. VNIGNI*, 1974, no. 152, pp. 194–214.

Sazonova, I.G. and Sazonov, N.T., The Berriasian Sediments in Boreal Provinces of Europe, *Bull. Mosk. Ob-va Ispyt. Prir., Otd. Geol.*, 1984, vol. 59, no. 1, pp. 86–98.

Shchennikova, A.S. and Arkad'ev, V.V., Tintinnides (Tintinnoidae, Infusoria) from Tithonian-Berriasian Sediemnts of the Mountain Crimea, in *Materialy LV Sess. Paleontol. Ob-va pri RAN* (Proc. LV Sess. of Paleontol. Soc. of RAS), St. Petersburg, 2009, pp. 166–167.

Smirnova, T.N., Lower Cretaceous Brachiopod Distribution in Crimea and Northern Caucasus, *Bull. Mosk. Ob-va Ispyt. Prir., Otd. Geol.*, 1962, vol. 35, no. 6, p. 132.

Sokolov, V.D., Materials on the Crimea Geology. The Crimea Tithonian, *Izv. Mosk. Ob-va Lyubitelei Estestvoznaniya, Antropologii i Etnografii*, 1886, vol. 14, pp. 1–43.

Tesakova, E.M., Savel'eva, Yu.N., and Arkad'ev, V.V., Tithonian and Berriasian Ostracods in the Eastern Crimea, in *Tez. Nauch. Konf. "Lomonosovskie chteniya"* (Proc. Sci. Lomonosov Conf.), Moscow: MGU, 2004.

Tesakova, E.M. and Savel'eva, Yu.N., Ostracods from Jurassic-Cretaceous Boundary Layers of the Eastern Crimea: Stratigraphy and Paleoecology, in *Paleobiologiya i detal'naya stratigrafiya fanerozoya* (The Phanerozoic Paleobiology and Detailed Stratigraphy), Moscow: Izd. MGU, 2005, pp. 135–155.

Yampol'skaya, O.B., Baraboshkin, E.Yu., Guzhikov, A.Yu., et al., Lower Cretaceous Paleomagnetic Section of the South-West Crimea, *Vestn. MGU, Ser. Geol.*, 2006, no. 1, pp. 3–15.

Yampol'skaya, O.B., Guzhikov, A.Yu., Baraboshkin, E.Yu., and Bagaeva, M.I., Magnetostratigraphic Characteristics of Jurassic-Cretaceous Sediments of the Eastern Crimea in *Yurskaya sistema Rossii: problemy stratigrafii i paleogeografii (23–27 sentyabrya 2009 g., Saratov)* (Jurassic System of Russia: Problems of Stratigraphy and Paleogeography. Proc. IV All-Russian Conf. September 23–27, 2009) Zakharov, V.A. Ed., Saratov: Izd. Tsentr "Nauka", 2009, pp. 265–267.

Yanin, B.T. and Smirnova, T.N., Stratigraphic Distribution of Bivalves and Brachiopods in Berriasian-Valangian Sediments of Crimea, *Bull. MOIP. Otdel. Geol.*, 1981, vol. 56, no. 1, pp. 82–94.

Yanin, B.T. and Baraboshkin, E.Yu., Ichnofossils in Lower Cretaceous Sediments of Crimea: Taxonomic, Stratigraphic, and Ichnofacial Analyses, in *Materialy 5-go Vseross. Soveshch. "Melovaya sistema Rossii i blizhnego zarubezh'ya: problemy stratigrafii i paleogeografii"* (Cretaceous System of Russia and Russia's neighboring states. Proc. V All-Russian Conf.) Baraboshkin, E.Yu. and Blagoveshchenskii, I.V., Eds., Ul'yanovsk: UlGU, 2010, pp. 364–366.